



Dynamical memristors for higher-complexity neuromorphic computing

Suhas Kumar¹✉, Xinxin Wang², John Paul Strachan^{3,4}, Yuchao Yang¹^{5,6}✉ and Wei D. Lu¹²✉

Abstract | Research on electronic devices and materials is currently driven by both the slowing down of transistor scaling and the exponential growth of computing needs, which make present digital computing increasingly capacity-limited and power-limited. A promising alternative approach consists in performing computing based on intrinsic device dynamics, such that each device functionally replaces elaborate digital circuits, leading to adaptive ‘complex computing’. Memristors are a class of devices that naturally embody higher-order dynamics through their internal electrophysical processes. In this Review, we discuss how novel material properties enable complex dynamics and define different orders of complexity in memristor devices and systems. These native complex dynamics at the device level enable new computing architectures, such as brain-inspired neuromorphic systems, which offer both high energy efficiency and high computing capacity.

The crisis in modern computing

Since the 1960s, the computing industry has striven to build larger numbers of smaller transistors on digital integrated chips to increase speed and functional density. Transistor densities have continued to double roughly every 2 years, a trend known as Moore’s law¹, but improvements in computing speed and capacity started saturating around 2006 (REF.²). This issue developed as chips grew in capacity and the data movement across distinct storage and processing units in the von Neumann architecture increased. Combined with the disproportionate progress in compute versus memory performance, this phenomenon, commonly known as the memory wall, leads to saturated system performance. Another serious impending issue is the end of practical size scaling as transistor dimensions approach atomic sizes. Hence, further advancements in computing speed and capacity face significant challenges.

¹Sandia National Laboratories, Livermore, CA, USA.

²Electrical Engineering and Computer Science Department, University of Michigan, Ann Arbor, MI, USA.

³Peter Grünberg Institute (PGI-14), Forschungszentrum Jülich GmbH, Jülich, Germany.

⁴RWTH Aachen University, Aachen, Germany.

⁵School of Integrated Circuits, Center for Brain Inspired Chips, Institute for Artificial Intelligence, Peking University, Beijing, China.

⁶Center for Brain Inspired Intelligence, Chinese Institute for Brain Research (CIBR), Beijing, China.

✉e-mail:
su1@alumni.stanford.edu;
yuchao.yang@pku.edu.cn;
wluee@umich.edu

<https://doi.org/10.1038/s41578-022-00434-z>

computers^{7,8}, while niche applications, such as edge artificial intelligence, suffer from the high costs and high power consumption of today’s digital solutions.

Over the next decade, Moore’s law can still be sustained, partly via increased device densities, but mostly through effective functional scaling via heterogeneous and 3D integration⁹. To continue this trend of functional scaling, advances in computing need to be achieved not by increasing device density but by packing more functional intelligence per volume of material^{12,10}. Thus, the engineering of smart materials and devices, and the invention of new architectures to efficiently utilize them, will be central to the post-Moore computing landscape.

The advent of bio-inspired computing

Since around 2006, there has been a clear realization of the urgency for a ‘post-CMOS (complementary metal-oxide-semiconductor)’ computing paradigm — one that circumvents the need for shrinking devices, dismantles the storage–processing divide (the von Neumann bottleneck) and overcomes the limitations of digital information processing^{11–13}. As a result, there was an explosion of ideas for post-CMOS computing, including some that were studied decades ago^{14–21} and non-electronic approaches, such as optical, quantum and biomolecular computing^{22–29}.

Within this Cambrian era of post-CMOS computing, there are strong arguments favouring bio-inspired (or brain-like/neuromorphic/neural) computing

approaches. High among those arguments is the remarkable energy efficiency and information-processing capabilities of all levels of biological organisms, from cells to the brain³⁰. Thus, reverse-engineering biological computing may offer the most mature, widely applicable and scalable approach^{31,32}. The 1940s witnessed the first efforts to model problem-solving biological neural networks and to mimic them using electrical circuits^{33,34}. Since then, there were periodic and consequential developments in this area: Hebbian learning¹⁴, neuron models (such as the Hodgkin–Huxley model)^{35–37}, the perceptron¹⁵, multilayer networks^{16,17}, backpropagation training^{18,19}, the Hopfield network²⁰ and self-organizing maps²¹, to name just a few. By the late 1980s, bio-inspired computing became a small but independent research area³⁸ and gained commercial traction in the early 2010s as a set of predominantly algorithmic tools^{39,40}.

Complexity and adaptation

The next frontier in advancing computing performance needs to incorporate the dynamical and adaptive capabilities of natural and biological systems (FIG. 1a). Biological systems at all levels respond to their environment and history. Simple molecular systems, such as nucleic acids, can express adaptive behaviours, including replication and self-repair, triggered by the local environment. Neurons, the core information-processing elements in biological systems, express over 20 different dynamical behaviours driven by electrochemical stimulation from their history and environment⁴¹. Similarly, systems with more organizational complexity, such as the eye and immune systems, and all the way up to organisms, express proportionally higher functional complexity and adaptation. By contrast, modern computing systems are built on top of static elements with zeroth-order complexity (see definitions below, FIG. 1b).

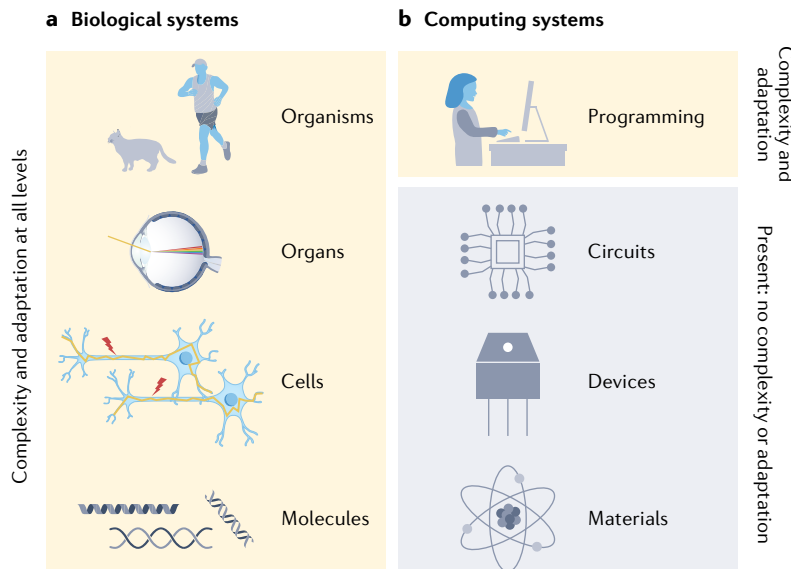


Fig. 1 | Biological and computational adaptation and complexity. **a** | Complexity and the resulting adaptation appear at all levels of biological organization, illustrated here with hierarchical systems and their expressions. **b** | In the hierarchy of current computer stacks, nearly all layers are unintelligent and contain no adaptation or complexity, and intelligence is provided by the programmer encoding the software.

Devices and circuits primarily transform inputs to new outputs, following prescribed logic tables, mathematical functions and conditional branching rules that are formulated by a biological system at the top: the human programmer. This computing system can show universal Turing completeness (assuming unlimited memory and time) and, thus, simulate the computational capabilities of an idealized Turing machine⁴². Yet, this system is a tool, dependent on the human programmer to wield it appropriately, dynamically adapting the instructions based on past (possibly mistaken) outputs and new demands from the environment.

The first breakthrough away from the above paradigm has been in the field of artificial neural networks (ANNs), particularly deep learning^{39,40}. Training an ANN to perform a task, such as image recognition, no longer uses traditional programming but is instead based on providing labelled examples to the network. Through dynamical updates of the network weights, guided by training algorithms (such as back-propagation), a form of adaptation and learning occurs. Significantly, this approach has brought adaptation and complex dynamics to a level below the user, at the algorithmic layer, eliminating explicit instruction programming. This approach has led to state-of-the-art capabilities in many computing tasks. The underlying hardware, however, remains static and low in complexity during both the training and the learning phases, and in the subsequent deployment of the ANN in performing inference on inputs. The next breakthrough will come from incorporating a capability for adaptation and complex dynamics within the hardware layers themselves. This idea offers an exciting path to increased computational parallelism, scalability (such as from mobile electronics to supercomputers), higher energy efficiency and an increased robustness to hardware and environmental variability and defects.

We invoke the concept of complexity throughout this discussion. Generally speaking, complexity is a set of interacting processes expressing a non-trivial behaviour, which has been defined in many ways across different disciplines^{43–46}. In other words, complexity is a measure of the dimensionality of a dynamical system. For our purposes, the measure ('order') of complexity is the number of first-order differential equations (or equivalent) required to describe the system's behaviour, each equation associated with a 'state variable' and its dynamical evolution^{46,47}. We stress that both the system's observed temporal dynamics and the internal state variables can be used to describe the system's adaptability, in response to both local stimuli and the system's history.

Expressions of higher-order complexity

Complexity appears at many levels from the microscale to the macroscale: within biological organisms^{48,49}, chemical processes^{50,51}, economic institutions^{52,53}, social organizations^{54,55}, ecological processes⁵⁰ and so on. As an illustration of different orders of complexity, a simple pendulum (a system with second-order complexity) exhibiting periodic oscillations can be easily modelled, but the weather system, which expresses chaos and stochasticity, is much higher in complexity and, thus, very difficult to model and predict. There are

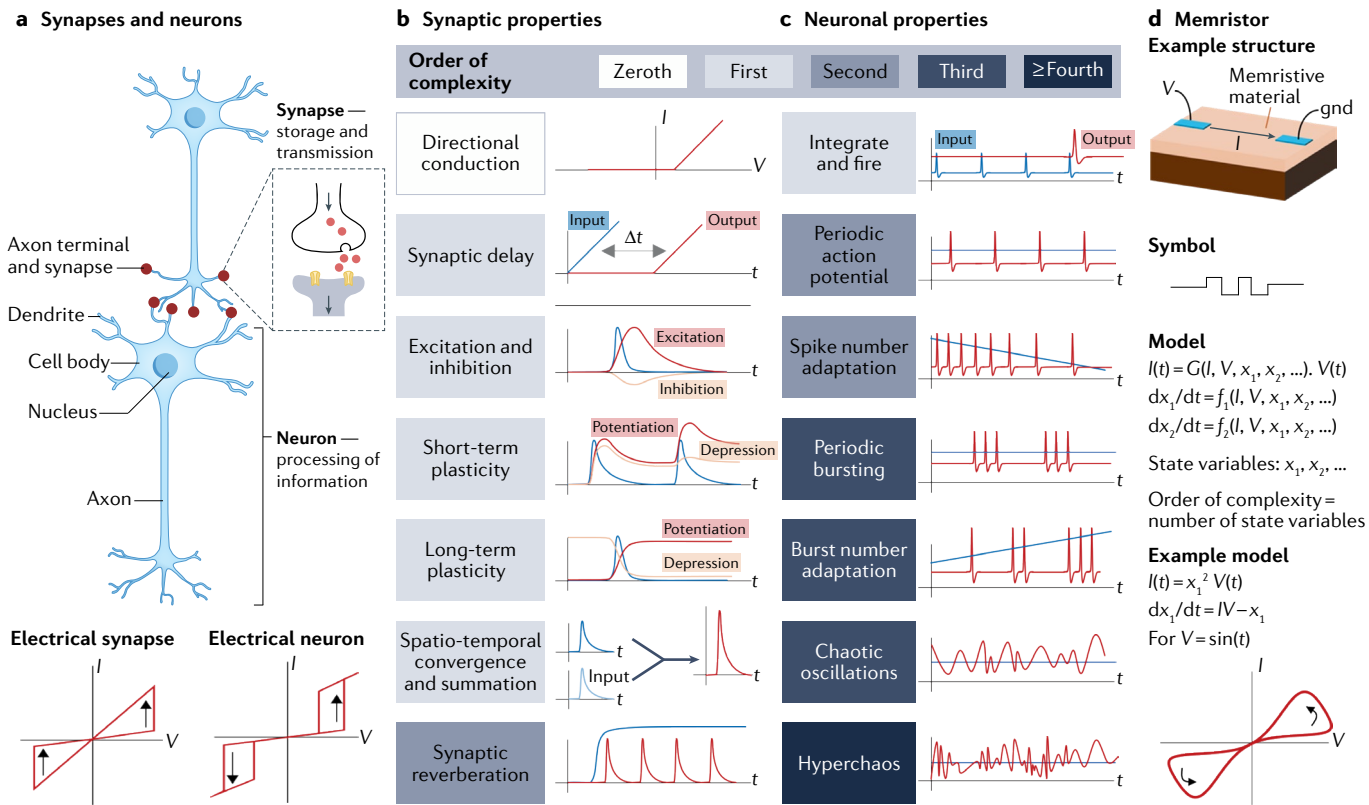


Fig. 2 | Concept of memristor and memristive behaviours of various complexity. **a** | Illustrations of a biological neuron and synapses, along with the current–voltage characteristics of synaptic and neuronal electrical devices. **b, c** | Examples of synaptic (panel **b**) and neuronal (panel **c**) behaviours that require different orders of complexity. **d** | Illustration of a memristor and its basic model, depicting with an example how state variables connect currents and voltages with a temporal history dependence. Δt , time delay; G , conductance; gnd, electrical ground; I , current; t , time; V , voltage.

many examples of biomimetic behaviours arising from electrophysico-chemical processes of different orders of complexities^{56–59}. Here, we start by reviewing illustrative examples of simple electrical and mechanical systems of different orders of complexity, before transitioning to specific biomimetic examples.

Zeroth-order systems, which effectively have no complexity, faithfully follow any input variations without adding a temporal component (such as a time delay). No real-world system is perfectly zeroth order. A massless object subject to finite friction is a zeroth-order system: its velocity temporally follows the applied force. In the electrical world, a pure resistor is a zeroth-order system: its current output faithfully follows the voltage input.

First-order systems are determined by a single first-order differential equation. A finite mass subjected to finite friction (state variable: velocity) reacts to an applied force with a time delay owing to friction. In the electrical world, a circuit with a resistance and capacitance reacts with its characteristic time constant (the ‘RC’ time constant). A time delay requires first-order complexity.

Second-order systems require two distinct and interdependent state variables, represented by two first-order (or an equivalent second-order) differential equations to describe their respective dynamics. A finite mass held by a spring (state variables: velocity and displacement) reacts to an initial finite displacement with oscillations in its displacement. In the electrical world, a circuit with

a resistance, inductance and capacitance reacts with damped oscillations to an input voltage pulse. Oscillatory behaviour requires at least second-order complexity^{46,60}.

A double pendulum is a fourth-order system (state variables: velocity and displacement, for each of the pendula) that produces chaotic dynamics in response to an initial displacement. Chaos and multiperiod oscillations require third-order complexity, while hyperchaos requires fourth-order complexity^{61,62}. Intuitively, chaos consists of hard-to-predict oscillations and, thus, requires an order of complexity higher than oscillations, whereas hyperchaos is hard-to-predict chaos and, thus, requires an order of complexity higher than chaos.

Below, we provide selected examples of different synaptic and neuronal functions of different orders of complexity. At a broad basic level, synapses store weights and modulate information transmission, whereas neurons perform non-linear transformations on their inputs (such as thresholding)⁶³ (FIG. 2a). The biological origins of these functions (such as ion channel dynamics) and their equivalent electrical and mathematical models have been extensively discussed in the literature^{35–37,41,63,64}.

Synaptic functions. Synaptic functions are summarized in FIG. 2b and include the following.

- Directional conduction (zeroth order): necessitates conductance to be asymmetrical with the polarity of the applied voltage. This behaviour requires no complexity.

- Synaptic delay (first order): produces a specific time delay between input and output. Recall that a time delay requires first-order complexity.
- Excitation and inhibition (first order): in response to an input stimulus, the output is either increased (excitation) or decreased (inhibition), depending on the state of the synapse. Usually, a temporal component such as a characteristic timescale is involved, invoking first-order complexity.
- Short-term plasticity (first order): the response to a temporal input (such as a spike) persists for a finite time before decaying to its pre-input value. Repeated temporal inputs lead to continually increased (potentiation) or decreased (depression) response. The memory period is determined by a characteristic timescale, invoking first-order complexity, whereas potentiation and depression behaviours can be captured via parameters within the same dynamical process, that is, they do not add complexity.
- Long-term plasticity (first order): the response to a temporal input (such as a spike) persists for practically an infinite time, either via potentiation or depression. The temporal persistence of the output requires a timescale, thus invoking first-order complexity.
- Spatio-temporal convergence and summation (first order): incoming signals from different channels are summed, involving a characteristic timescale, thus invoking first-order complexity.
- Synaptic reverberation (second order): in response to a stimulus, oscillations may result from feedback-enabled synaptic structures. The feedback and the time delays create two distinct dynamical processes, which together result in second-order complexity.

Neuronal functions. Neuronal functions are summarized in FIG. 2c and include the following.

- Integrate and fire (first order): neurons accumulate potential from multiple temporal inputs for a finite time and, when the accumulated potential exceeds a threshold, they produce a temporal output. Similar to short-term potentiation in synapses, this process essentially invokes a delay-like first-order complexity.
- Periodic action potential (second order): in response to a constant input, neurons can produce periodic spikes, also known as action potentials. Recall that any oscillatory behaviour requires second-order complexity.
- Spike number adaptation (second order): this process is similar to the one producing periodic action potentials (second-order complexity) but with an additional parameter that modulates the frequency as a function of the input level.
- Periodic bursting (third order): in response to a constant input, neurons can produce periodic bursts of spikes. Recall that multiperiod oscillations require third-order complexity (such as for a driven simple pendulum).
- Burst number adaptation (third order): this process is similar to the one producing periodic bursting (third-order complexity) but with an additional parameter that modulates the number of spikes within each burst as a function of the input level.

- Chaotic oscillations (third order): neurons can produce chaotic dynamics in response to a constant input, which, in simple terms, is a deterministic (non-random) behaviour that is hard to track. Recall that chaotic dynamics requires third-order complexity.
- Hyperchaos (fourth order): technically, hyperchaos is a behaviour containing at least two Lyapunov exponents, which, in simple terms, means that it is much harder to track than chaos. Sometimes, neural systems produce hyperchaos, which requires fourth-order complexity⁶⁵.

From these few examples of synaptic and neuronal behaviours, it is apparent that neuronal functions are often higher in complexity. This agrees with intuition, because, from a computing point of view, the main function of neurons is to perform temporal processing of information, whereas synapses store information. Temporal expressions are more complex, by definition.

Memristors and complexity in computing

Most efforts into bio-inspired computing thus far have focused on mimicking primitive lower-order biological complexities. Historically, such complexities are emulated using transistor-based circuits (such as central and graphics processing units, CPUs and GPUs) to simulate multiple dynamical equations^{2,66,67}, but recent advances in memristors have made this approach easier.

Memristors, predicted in 1971 (REF.⁶⁸) and connected to physical devices in 2008 (REF.⁶⁹), are electrical circuit elements that embody at least one state equation (differential equation of the state variable with respect to time) and, thus, at least first-order complexity (FIG. 2d). The incorporation of state equations necessarily leads to history-dependent behaviours in the current–voltage plot, in either volatile (memory disappears at zero bias) or non-volatile (memory is retained at zero bias) form. Processes such as temperature-driven Mott transitions⁷⁰ and field-driven defect generation and recombination⁷¹ lead to volatile or sometimes partially volatile memory effects⁷². By contrast, processes such as electrochemical defect migration⁷³, spin injection^{22,74}, ferroelectric or ferromagnetic switching^{75,76} and crystalline–amorphous phase transitions⁷⁷ lead to non-volatile memory effects, and are all captured within the memristor framework.

Non-volatile (or partially non-volatile) memristors are good candidates as electrical synapses, offering tunable weight and non-volatile memory, wherein the output current is the conductance-weighted input voltage. Volatile memristors perform a non-linear transformation of the input, such as thresholding, and are, thus, excellent candidates for electrical neurons. Further, volatile memristors are often capable of generating neuron-like temporal dynamics of higher-order complexity, as discussed in the following sections.

Thus, unlike transistor-based hardware that simulates biomimetic functions using many devices, memristors naturally embody simple biomimetic functions. Therefore, since around 2013, there has been a flurry of research into bio-inspired computing systems based on simple (low-complexity) memristor functions, which promise far greater efficiencies than CPUs and

Synaptic devices			
	a First order	b Second order	c Second order
Materials and structures			
Proposed mechanism	Movement of oxygen defects	O ⁺ vacancy filament formation	Ferroelectric defect response
State variables	<ul style="list-style-type: none"> Width of oxygen gradient 	<ul style="list-style-type: none"> Filament conductance Temperature 	<ul style="list-style-type: none"> Built-in electric fields Frequency response of defects
Behaviours of a single device	<p>Non-volatile resistance switching</p>	<p>Non-volatile resistance switching and dynamical memory</p>	<p>Non-volatile resistance and polarization switching and dynamical memory</p>
Neuronal devices			
	d First order	e Second order	f Third order
Materials and structures			
Proposed mechanism	Joule heating and electrical non-linearities	Mott transition, filament formation	Dynamics of Mott transition, temperature and charge
State variables	<ul style="list-style-type: none"> Internal temperature 	<ul style="list-style-type: none"> Temperature Charge on internal capacitor 	<ul style="list-style-type: none"> Temperature Charge on internal capacitor Speed of Mott transition
Behaviours of a single device	<p>Volatile resistance switching</p>	<p>Volatile resistance switching and self-oscillations</p>	<p>Volatile resistance switching and 15 types of neuron-like dynamics</p>

Fig. 3 | Examples of memristors of different orders of complexity. Examples of synaptic (panels **a–c**) and neuronal (panels **d–f**) memristive devices with different orders of complexity. The switching mechanism, state variables and typical device characteristics are indicated. **a** | TiO_2 sandwiched between Pt electrodes exhibits dynamics in the width (w) of a conducting filament in response to a train of voltage pulses (V), resulting in temporal non-volatile changes to its conductance (G). **b** | Two different oxides of Ta sandwiched between Pt electrodes exhibit dynamics in the conductance of a filament and the local temperature (T) in response to a train of voltage pulses, resulting in temporal non-volatile changes to its conductance. **c** | Ferroelectric HfZrO_x sandwiched between TiN and Si electrodes exhibits dynamics in the built-in electric field (E) and the frequency response of defects (F) in response to a train of voltage pulses, resulting in temporal non-volatile changes to its conductance. **d** | TiO_2 sandwiched between Ti/Pt and Pt undergoes a non-linear steady-state change in internal temperature in response to an applied current (I) and voltage (V), leading to negative differential resistance in the I – V characteristic. **e** | NbO_2 sandwiched between Pt electrodes, which contains a built-in capacitor, exhibits self-oscillations in voltage when under optimally fixed bias conditions. **f** | A special device structure containing NbO_2 as the active material enables coexisting dynamics in three state variables, leading to several tunable neuron-like behaviours in current (I) dynamics. Periodic spiking (in blue) and periodic burst spiking (in red) are displayed. t , temperature. Panel **a** adapted from REF.⁶⁹, Springer Nature Limited. Panel **b** adapted with permission from REF.¹¹, ACS. Panel **c** adapted with permission from REF.¹¹³, ACS. Panel **e** adapted with permission from REF.¹¹⁷, Wiley. Panel **f** adapted from REF.⁴⁷, Springer Nature Limited.

among such devices can lead to higher-level capabilities and energy efficiency (that is, system-level complexity). This idea is the bedrock principle for complexity in computing, including higher-complexity bio-inspired computing.

Memristors of different complexities

In this section, we provide various examples of synaptic and neuronal memristors of different orders of complexity and point to their working mechanisms. There are many comprehensive recent reviews on simple (low-complexity) memristive switching materials, mechanisms and device-level performance^{90,99–104}, including special material classes, such as 2D materials^{85,105,106}, Mott insulators¹⁰⁷, organic materials^{108,109} and carbon nanomaterials¹¹⁰. Here, instead, we focus on higher-complexity memristive materials and devices and discuss how complex computing can be achieved by taking advantage of the intrinsic device dynamics. A few representative examples that illustrate complexity beyond the simple (and often static) functions that can be engineered in memristive electronic devices are summarized in FIG. 3.

Synaptic devices

First-order synaptic memristors. The first experimentally identified memristor was a first-order memristor⁶⁹ (FIG. 3a). The switching mechanism was based on the movement of oxygen vacancies in TiO_2 in an electric

GPUs^{78–98}. Although exploration of memristors with higher-order complexity has just begun, it is clear that it is indeed possible to engineer qualitatively highly complex behaviours (especially biomimetic) from interacting electro-physico-chemical material processes in memristors. As a consequence, a single device with such complex behaviours can functionally replace hundreds or thousands of transistors, and interactions

field. The width of the TiO_2 region occupied by the oxygen defects was the proposed state variable. The device exhibited non-volatile resistance switching.

Most memristors or two-terminal memory devices ever built are first-order memristors. They all exhibit some form of non-volatile information storage with minimal temporal dynamics and invoke one dominant dynamical process that enables storage. Although many of them may have additional state variables (for instance, temperature dynamics are present in every electronic device), for simple information storage — the default behaviour explored in most memristors — only one dynamical process is required (first-order complexity). Because of that, it is important to note that many first-order memristors exhibit higher-order functions when the appropriate measurements are used to observe the additional dynamics.

Second-order synaptic memristors. Memristors based on TaO_x (REF.¹¹¹) were designed to be sensitive to thermal effects (FIG. 3b). Two state variables were identified: the radius of a filament of oxygen vacancies (which determined the resistance) and temperature (the dynamics of which depend on the thermal environment of the device and its operating conditions). The device exhibited dynamical (temporal) memory in addition to the usual static non-volatile resistance switching. Similarly, in HfO_2 memristors, possible fingerprints of second-order effects were identified¹¹², especially temporal memory.

In ferroelectric memristors, two state variables were identified¹¹³: built-in electric fields and the dynamical response of the interfacial defects (FIG. 3c). Similar to the previous examples, this memristor exhibited temporal memory in addition to the usual resistance switching behaviour (accompanying the expected polarization switching in a ferroelectric material). Besides these examples, there have been few confirmed examples of second-order synaptic memristors.

Neuronal devices

First-order neuronal memristors. First-order neuronal memristors essentially exhibit volatile switching in the current–voltage plane and some simple dynamics (such as a characteristic response time). In the field of computer memory, selector devices, which are essentially volatile switches that minimize low-bias current leakage, have been intensely researched for over a decade^{114,115}. Thus, most selectors can be considered neuronal memristors of at least first-order complexity. Many mechanisms can lead to volatile switching (Mott transition, thermal runaway, volatile defect migration, tunnelling and more). For example, modelling of threshold switching in TiO_2 as a first-order process with internal temperature as the state variable¹¹⁶ showed that, as temperature increases due to Joule heating, the superlinear temperature dependence of the conductance makes the conductance increase, which, above a threshold, is a runaway process, leading to volatile (reversible) switching. Interestingly, in this range, either the current rapidly increases at a held voltage or the voltage drops at a held current (current-controlled negative differential resistance, FIG. 3d). Although it is possible that first-order memristors that exhibit volatile

memory or hysteresis may exhibit oscillations or other higher-order functions, such measurements were not of interest for their intended applications.

Second-order neuronal memristors. Volatile memristors placed in a relaxation oscillator circuit can exhibit self-sustained oscillations. For example, volatile memristors (exhibiting current-controlled negative differential resistance) with a parallel capacitor can exhibit oscillations via two alternating dynamical processes: charging–discharging of the capacitor and volatile switching of the memristor, thus exhibiting second-order complexity. The electrode structure of a NbO_2 volatile-switching memristor was shown to form a built-in capacitor, which was sufficient to create oscillations without the need for any external capacitor¹¹⁷ (FIG. 3e). The device was modelled with a Mott-transition-driven volatile filament (conduction channel) formation process, although later models were based on more realistic and general thermal runaway processes⁴⁷. Such oscillatory behaviour from a single device has been observed several times since then, though it has been identified as a second-order memristive effect very few times.

Third-order neuronal memristors. The only reported third-order memristor⁴⁷ was constructed using NbO_2 and modelled with three state variables: temperature (representing internal thermal dynamics), charge on the built-in capacitor (representing charge dynamics) and the speed of formation of a metallic region (a volatile filament resulting from the Mott transition dynamics, FIG. 3f). The devices were carefully designed in structure and material stoichiometry to enable all the above dynamics. When powered by a tunable static voltage input, a single device could produce 15 different neuronal dynamics (including spiking, bursting and chaos).

Although third-order complexity can produce many key neuronal behaviours, a rigorous mathematical examination of common neuronal models is needed to evaluate whether higher-order complexity is required to faithfully emulate a neuron. For example, the common Hodgkin–Huxley neuron model involves fourth-order complexity, but most behaviours of a Hodgkin–Huxley neuron can be produced by a third-order system, as discussed above³⁵. Models with fifth-order complexity have also been utilized to explain certain neuronal behaviours, but may be equivalently represented by lower-order dynamics¹¹⁸.

Emulation of higher-order functions using multiple circuit elements

A single memristor that exhibits fourth-order or higher-order dynamics has not been experimentally reported. As in most scientific studies, low-cost simulations often precede experimental demonstrations. In electronic device research, realistic emulations of specific functions are commonly performed using multi-component circuits or programmable hardware (such as field-programmable gate arrays). Such research evaluates a large parameter space at a reasonable cost, while invoking some experimental constraints (unlike in pure mathematical models) to allow the resulting parameters

to strategically inform materials engineering, which eventually leads to the desired higher-order devices.

A common example of such emulation in neuronal memristor research is the generation of second-order neuron-like oscillations (similar to those discussed in the subsection on second-order neuronal memristors), but with distinctly different components (a distinct parallel capacitor and a series resistor, for example) instead of a single second-order component¹¹⁹.

A non-transistor fourth-order memristive system was constructed¹²⁰ using two volatile first-order VO_2 memristors to emulate a Hodgkin–Huxley-like neuron model (FIG. 4a). The state variables were the internal temperatures of the memristors and the charges on their parallel capacitors. The system produced 23 different neuronal functions, such as spiking, bursting and integrate-and-fire. Although, in principle, a third-order system could have produced all those functions, the engineering of the circuit was easier and more flexible (for example, for obtaining the precise bias) with fourth-order complexity.

In another example, a transistor-based fourth-order memristive-like system was constructed using transistor-based active components (amplifiers) to

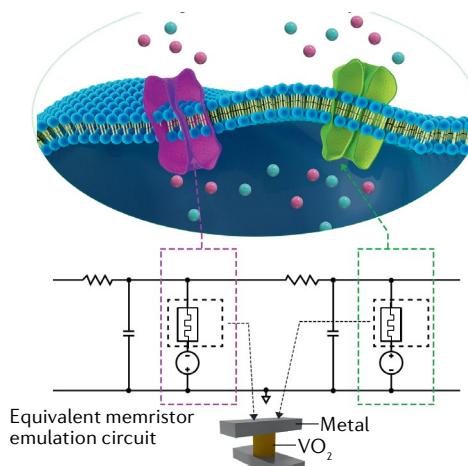
mimic memristors¹²¹ (FIG. 4b). The system produced hyperchaos, a fourth-order function.

There are several other higher-order and fractional-order simulations or emulations, including memristor-inspired ones, generating complex functions such as chaos or hyperchaos^{122–127}. Additional orders of complexity are useful only if they are required to enable a specific behaviour or if they clearly make the system design easier (as in the previous example). For instance, the simulation of ninth-order circuits capable of producing hyperchaos has been reported, demonstrating advanced circuit simulation capabilities, although hyperchaos only requires fourth-order complexity¹²⁸.

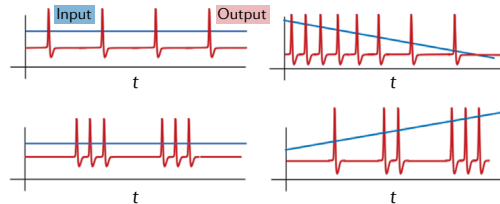
Creating complexity in computing using memristors

As we discussed, most efforts in memristor-based bio-inspired computing have, thus far, centred around mimicking simple (low-complexity) synaptic and neuronal functions using static memristive properties or primitive first-order dynamics (such as dynamical plasticity). Such efforts have been covered in several reviews^{78–98,129,130}. In this section, we briefly illustrate examples (FIG. 5) of how memristors of different

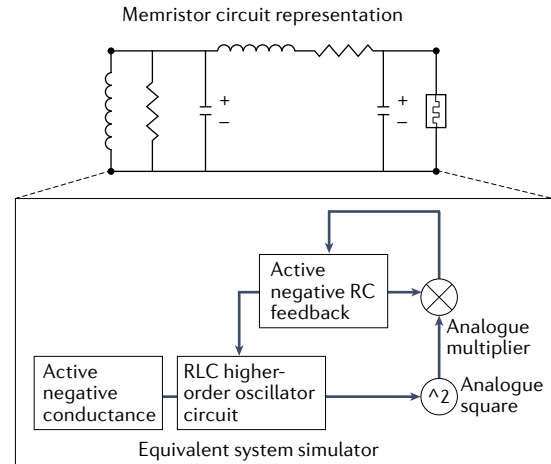
a Non-transistor fourth-order memristive system



Key result: 23 neuron-like behaviours



b Transistor-based fourth-order memristive system simulator



Key result: hyperchaos

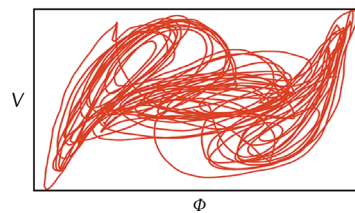


Fig. 4 | Emulation of higher-order complexity using multiple circuit elements. **a** | Emulation of higher-order complexity using a memristor-based biomimetic circuit. The structure of a neuron's membrane on which Na (pink) and K (green) channels modulate the flow of Na and K ions (free-floating pink and bluish-green spheres, respectively) is illustrated. The behaviour of Na and K channels leading to neuronal dynamics is emulated using the illustrated memristor circuit that contains fourth-order complexity (the two VO_2 memristors and the two capacitors, each supplying one state variable). Twenty-three neuronal dynamics were emulated using this circuit. Four of them are illustrated (periodic action potential, spike number adaptation, periodic bursting and burst number adaptation). **b** | Emulation of fourth-order complexity using transistor-based circuit elements. The circuit produced hyperchaos, a highly irregular and unpredictable behaviour, as illustrated in the plot of voltage (V) against phase (ϕ). RC, resistance–capacitance; RLC, resistance–inductance–capacitance; t , time. Panel **a** adapted from REF.¹²⁰, CC BY 4.0. Panel **b** adapted with permission from REF.¹²¹, World Scientific.

(especially higher-order) complexities can solve problems that would otherwise require increasingly elaborate circuits, depending on the complexity of the problem.

Information processing with static properties

Most current studies on memristor-based computing systems do not invoke any dynamics but merely program an array of memristors to target resistances and

use it as a system of synapses to perform computations. An approach widely used over the past 5 years consists of programming crossbar arrays of memristors (as in REF.¹³¹) to represent patterns and make the network perform multiplication of an input voltage vector with the matrix of memristor conductances to produce a vector of currents (vector–matrix multiplication, VMM, FIG. 5a). VMMs enable convolutions, which lead to the

Using memristors with different orders of complexity for computing

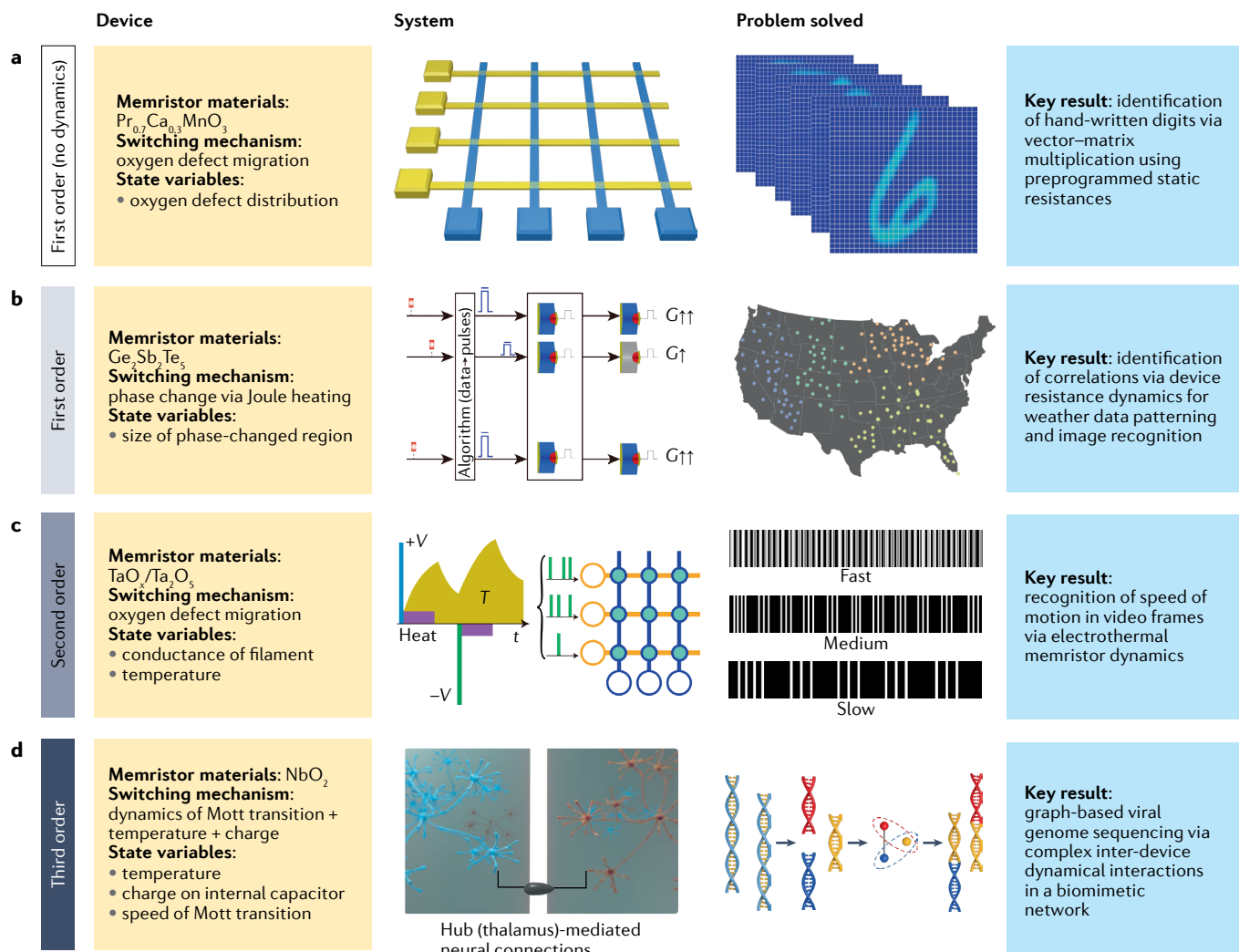


Fig. 5 | Computing with memristors of different orders of complexity.

Typical device structures and their corresponding computing systems and applications for memristive devices with first-order (without dynamics, panel a), first-order (with intrinsic dynamics, panel b), second-order (panel c) and third-order (panel d) complexity. a | Static resistances (representing hand-written digits) were programmed into a memristor crossbar array, which was used to perform single-step vector–matrix multiplications to achieve convolution of input voltage vectors with the stored resistance values, to achieve classification of the inputs as one of the pre-stored digits. b | Streams of data were fed into an array of memristors made of the phase-change material $\text{Ge}_2\text{Sb}_2\text{Te}_5$, via an algorithm that converts input data into voltage pulses, with temporally correlated streams assigned larger amplitudes. The resulting change in conductance (G) in the devices encoded the temporal correlations in the input ($G\uparrow$ represents a small increase in G and $G\uparrow\uparrow$ represents a large increase in G). When the input was weather data, the geographical–temporal correlations of the data could be

identified, as depicted by the similarly coloured points on a US map. c | TaO_x memristors are sensitive to both electric fields (V) and local temperature (T), with the thermal timescales being larger. When binary time-varying video frames were fed as inputs to an array of such memristors, the spatial frequency of the resulting resistance pattern across the array, influenced by the rate of input excitation and the inherent thermal timescales, reflected the speed (frequency) at which the video frames changed. d | NbO_2 oscillators networked similar to thalamocortical neurons align in groups of phases that represent a solution to the graph problem that their connections represent. When a viral genome sequencing problem was encoded as a graph problem and represented by the NbO_2 network, the network found the maximum cut of the graph, which represents a solution to the sequencing problem. t , temperature. Panel a adapted with permission from REF.¹³¹, IEEE. Panel b adapted from REF.¹³⁵, CC BY 4.0. Panel c adapted with permission from REF.¹³⁷, IEEE. Panel d adapted from REF.⁴⁷, Springer Nature Limited.

identification of closely matching patterns, useful, for instance, in object detection and classification, such as recognizing handwriting or speech¹²⁹. Besides convolutional neural networks, many other neural-network architectures, machine-learning algorithms and scientific computing tasks utilize static properties of memristors, including multilayer perceptrons, recurrent neural networks, *k*-means clustering and the solution of partial differential equations^{129,130,132}.

VMMs typically use static memristor properties, but the efficient training of such memristors (that is, programming their conductances based on an update rule) is far from mature, owing to non-idealities such as device variation, non-linear and asymmetrical conductance updates and endurance problems. Achieving efficient training, especially within the time and energy constraints imposed by many applications, may require understanding and exploiting the temporal dynamics (first-order properties) during the switching of a memristor's resistance^{2,98,133,134}.

Computing with first-order dynamics

Gradual changes in the resistance of GeSbTe were used to detect correlations in input data¹³⁵ (FIG. 5b). GeSbTe is a phase-change material, in which resistance changes occur owing to the gradually (and temporally) varying size of the crystalline structure upon Joule heating driven by electrical or optical power: a first-order process. An incoming data stream (such as from an input image) can be treated with a simple linear algorithm and then used to stimulate a network of phase-change memristors. Temporally correlated signals in the different channels of the incoming data stream are added to maximize the resistance change in the different memristors. Thereby, the spatial distribution of the channels with temporal correlations can be computed, opening up wide applications in pattern recognition and event mapping (such as weather mapping). Besides such resistance switching, the amorphous phase of GeSbTe or its derivatives (such as C-doped GeSbTe) is relatively unstable and can go through spontaneous structural relaxations and transform to a more stable glass state, which naturally leads to gradual conductance drift to lower conductance. This is also a first-order process and has been used as the eligibility trace for efficient reinforcement learning¹³⁶.

Computing with second-order dynamics

Memristors sensitive to thermal dynamics, similar to those reported in REF.¹¹¹ and discussed in the section on second-order synaptic memristors, were designed using TaO_x (REF.¹³⁷) (FIG. 5c). The memristors contained two dynamical processes (making them second order): oxygen vacancy migration (which modulated the resistance) and temperature decay following an electrical stimulus. The idea was to stimulate a network of second-order memristors with a temporally evolving input pattern, resulting in a spatial resistance pattern determined by the switching and thermal dynamics. The spatial frequency of the pattern was proportional to the temporal rate of input evolution (as demonstrated using a white pixel moving on a dark background). Thus, the

temporal dynamics of a spatially distributed input could be quantified.

Computing with third-order dynamics

The third-order memristor⁴⁷ discussed in the section on third-order neuronal memristors was used in a network with capacitive couplings, laid out in a bio-inspired architecture (FIG. 5d). The couplings among the third-order memristors defined a graph problem. The couplings resulted in a spatial segregation of the phases of the memristors' oscillatory dynamics, which represents the solution to the problem. Solutions to small-scale non-deterministic polynomial-time (NP)-hard viral genome sequencing (posed as graph problems) were demonstrated. Coupled oscillatory networks have clear biological inspirations. The synchronization of clusters of biological neurons is key to the generation of crucial rhythms of muscular and nervous systems, similar to how clocking works as a synchronization scheme in digital electronic chips. Coupled oscillatory systems are a more general class of computing systems with spatio-temporal complexity, as discussed further in the section on coupled oscillatory networks.

Simulations and emulations of higher-order computing systems

Although the manufacturing of higher-order memristors is in its infancy, there are many simulations and emulations of higher-order devices or systems and explorations of their computing applications. For example, there are a series of hyperchaotic fourth-order and higher-order systems (often memristor-inspired) that is shown, mostly via simulations, to enable data encryption (such as images) and secure communication^{123–126}. Polynomial-time (but exponential-resource) solutions to NP-hard problems were demonstrated via chaotic dynamics in third-order and higher-order systems¹²².

Thus, low-cost simulations have favourably established the direction and motivation for materials research towards higher-order device complexity and computing applications. It is apparent that the theoretical exploration of this space is still limited, but we expect it to expand and grow alongside more experimental demonstrations of higher-order complex devices and their computing applications.

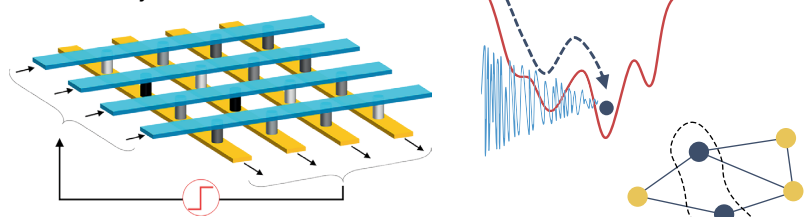
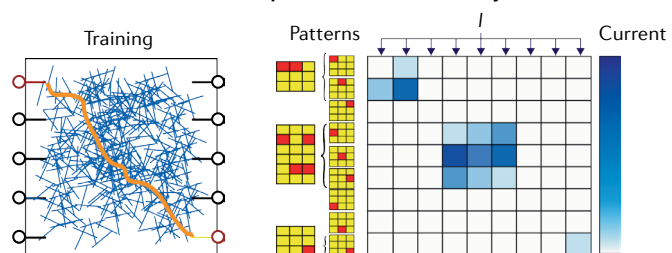
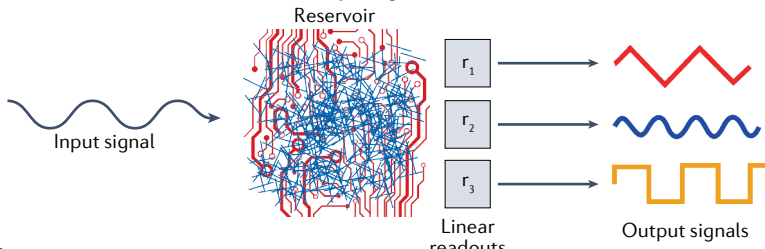
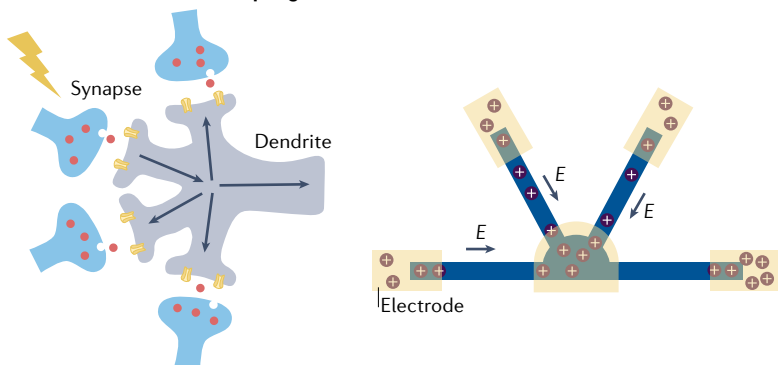
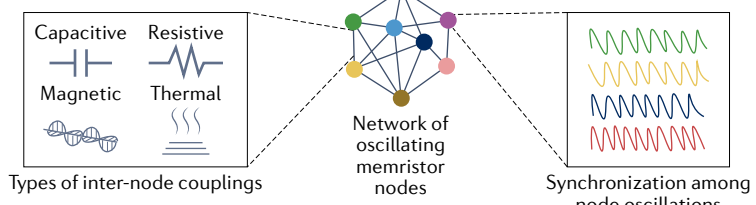
Spatio-temporal complexity

Complexity can be added to a device via new electro-physico-chemical dynamics, but it can also be achieved by enabling unique network dynamics via clever spatial connections among many devices (FIG. 6). We define this idea as spatio-temporal complexity.

Feedback

The simplest network-level spatio-temporal complexity is feedback of the outputs to the inputs, which creates recurrence and a temporal component, as illustrated with the following examples.

Fixed feedback was introduced in a VMM system made of a synaptic TaO_x memristor crossbar array¹³⁸

a Feedback dynamics**b Nanowire network — temporal associative memory****c Nanowire network — reservoir computing****d Inter-memristor ionic coupling****e Coupled oscillatory networks**

(FIG. 6a, left). The feedback implemented an Ising model (in the form of a Hopfield network) that converged to the minimum of a cost function associated with the programmed matrix (representing the problem), where the minimum represents the solution to the problem. The Ising model is a dynamical model that feeds the previous output into the input of the system. The Hopfield network was shown to solve NP-hard maximum-cut graph problems with efficiencies 10,000 times better than the best transistor-based approaches.

Fig. 6 | Computing based on spatio-temporal complexity of memristors.

a | Computing based on feedback dynamics in memristive arrays, where the feedback can be fixed (such as in Hopfield networks) or tunable. Both types of feedback enforce the minimization of a quantity associated with the matrix encoded in the memristive array's resistances, with the global minimum of the quantity usually representing the desired solution. Attaining such a global minimum, while escaping local minima, can be aided by controlled perturbations or noise that are inherent in memristors (illustrated as a blue noise signal aiding a solid grey circle find the global minimum in the red landscape). Such a minimization process can be used to solve optimization problems or differential equations. An optimization process is illustrated as finding the maximum cut of a graph (a cut of the set of vertices across the maximum number of edges, dashed curve). **b** | Randomly distributed nanowire network used as temporal associative memory, where the system creates volatile conduction pathways with an associated timescale (upon training with a target pattern), which enables matching of input patterns to the closest pattern within the training set (via high currents that form due to correlations). **c** | A reservoir computer using a mesh of memristive nanowires (blue wires) connecting a set of electrodes (red lines). Inputs are transformed into a higher-dimensional space, which can be used to perform classification tasks. A simple demonstration consists of producing signals of different frequencies or shapes depending on the input, as shown in the illustration.

d | A 'physically evolving network' that exploits the intrinsic dynamics of metal nanoclusters. The network emulates biological synapses that interface with neurons, wherein ionic migration and clustering can create both cooperative and competing changes to the synaptic weights. A similar idea can be implemented with ionic memristors, where the conductance between two electrodes can be modulated (up or down) by a third electrode, which was implemented in a multi-electrode system as illustrated. **e** | Networks of coupled memristor oscillators (spherical nodes in the network) based on resistive, capacitive, magnetic or thermal coupling (edges in the network). The synchronization among the phases of the oscillations of the different nodes (memristors) occurs based on the connection pattern, thereby solving a graph problem. E , electric field; I , current. Panel **a** adapted from REF.¹³⁸, Springer Nature Limited. Panel **b** adapted from REF.¹³⁹, CC BY 4.0. Panel **c** adapted with permission from REF.¹⁴⁰, IOP. Panel **d** adapted from REF.¹⁵⁴, Springer Nature Limited.

Tunable feedback was introduced in a VMM system made of a synaptic TaO_x memristor crossbar array (FIG. 6a, right). The system implemented the partial difference method of solving differential equations. This process involves iterative multiplications of intermediate solutions from a previous step, which was achieved by feeding back the previous VMM results to the input. The network was shown to solve the Poisson's equation and simulate fairly complex plasma systems, with the results agreeing with digital floating-point calculations.

Randomized nanowire networks

Several recent efforts have used networks of randomly distributed nanowires with memristive properties for computing, as illustrated in the examples below. Typically, the nanowires are metallic and are coated with

a memristive material, which makes the junction of two wires a synaptic switch.

A network of polymer-coated Ag nanowires was constructed, connecting a set of input–output electrodes¹³⁹ (FIG. 6b). Thus, when an input–output node pair was electrically stimulated, a unique metallic pathway between the node pair was established. The connections persisted for varying amounts of time, depending on the programming power and the path length (this creates a temporal component and, thus, complexity). This architecture enabled the identification of input patterns compared with a preprogrammed set of patterns, even when the input was slightly corrupted.

In a network of Ag₂S-coated Ag nanowires, Ag₂S switched in resistance via the movement of Ag ions¹⁴⁰ (FIG. 6c). The system was used to transform a temporally varying input to a higher-dimensional space, where the outputs at the different terminals were each a unique superposition of the input weighted and time-delayed to different extents (thereby introducing complexity). This system is known as a reservoir computing system. The different outputs, via linear combinations, could be used to classify previously indistinguishable lower-dimensional states and generate signals of different frequencies, a primitive but important signature of reservoir computing. Memristor-based nanowire networks have been the subject of several other studies as well^{141–150}. Reservoir computing systems have also been built with memristor networks that exhibit first-order neuronal dynamics (such as volatile memory), by using WO_x ionic memristors and spin memristors, for tasks such as image recognition, speech recognition and long-term forecasting of time-series data^{151–153}.

In nanowire networks, it is apparent that not every input terminal is directly connected to every output terminal but, instead, there are indirect connections. Such sparsity in connectivity is an attribute of biological neural networks and enables their massive scale². This idea can be adapted from nanowire networks to other computing systems.

Memristive devices with internal ionic coupling

Memristors were constructed with multilayered MoS₂ intercalated with Li⁺ ions, and the resistance switching mechanism was the movement of Li⁺ ions, which were otherwise stored in the inert Au electrodes, under an electric field. When multiple devices shared a common electrode¹⁵⁴ (FIG. 6d), this turned into a common source of Li⁺ ions. By using an appropriate sequence of programming of the different devices, two important biomimetic synaptic network behaviours were demonstrated: enhancement (cooperation) and decrease (competition) of conductance in multiple devices upon enhancing the conduction of one. Cooperative dynamics are an essential component of group behaviour, including decision-making and resource allocation. Implementing it requires elaborate digital circuits, which, in this case, are built into the spatio-temporal nature of the memristors.

A memristive ‘physically evolving network’ was also constructed¹⁵⁵, consisting of Ag nanoclusters embedded in a dielectric, such as amorphous Si or SiO₂, accessed

by multiple metallic electrodes. Under an electric field, there were electrochemical reactions and movements of the Ag nanoclusters, which behaved as bipolar electrodes and self-organized into conductive filaments. The location and strength of the conductive filaments formed by the electric field between two electrodes were modulated by the electric field applied by a third electrode, thereby expressing heterosynaptic plasticity. Heterosynaptic plasticity is a biological behaviour in which the synaptic strength between a pair of neurons depends on the activity at a third and different modulatory terminal. In the memristive evolving network, the concept of heterosynaptic plasticity via self-organization of nanoclusters was demonstrated in four-terminal memristive networks.

Coupled oscillatory networks

Similar to how two mechanically coupled pendula synchronize in phase, electronic oscillators also undergo synchronization when coupled. The phases of the oscillators map onto the couplings, effectively solving a graph-partitioning problem represented by the couplings. This idea has been developed into several sophisticated oscillator-based computing systems (FIG. 6e), where the oscillatory nodes can be implemented by self-sustained oscillators based on second-order VO₂ and NbO₂ memristors, spin-torque memristors and so on. The couplings are often capacitive (as in the example in the section on computing with third-order dynamics), resistive or magnetic; this topic is reviewed in depth in REF. ¹⁵⁶. Thermal couplings are also being explored¹⁵⁷. In the quantum world, quantum oscillators can be coupled via quantum energy exchange; they are popular platforms for scientific exploration, which also have strong computing potential^{158,159}.

Many recurrent static VMM networks (such as Hopfield networks)¹³⁸ and coupled oscillatory networks¹⁵⁶ are conceptually very similar. Remarkably, in the oscillatory networks, feedback and feedforward (for example, of phase information) are built into the same dual-direction hardware connections, enabled by the higher order of complexity. Recurrent VMM networks do not invoke device complexity and, thus, require an explicit feedback. Both systems operate via a ‘search’ process to converge towards the energy minimum, which, in the case of an associative memory, corresponds to a stored pattern closest to the input pattern and, in the case of optimization, corresponds to an optimized configuration of a graph problem (or another NP-hard optimization problem).

Additional physico-chemical memristor dynamics
In this section, we discuss several possible dynamical processes associated with new physics that is still being explored and that may add scientifically interesting and technologically useful complexities.

Non-equilibrium states in phase transitions

Although phase transitions have been extensively used for computer memories in storage units (such as the crystal structure transition in GeSbTe) or selectors (such as the Mott transition in NbO₂ and VO₂), the dynamics

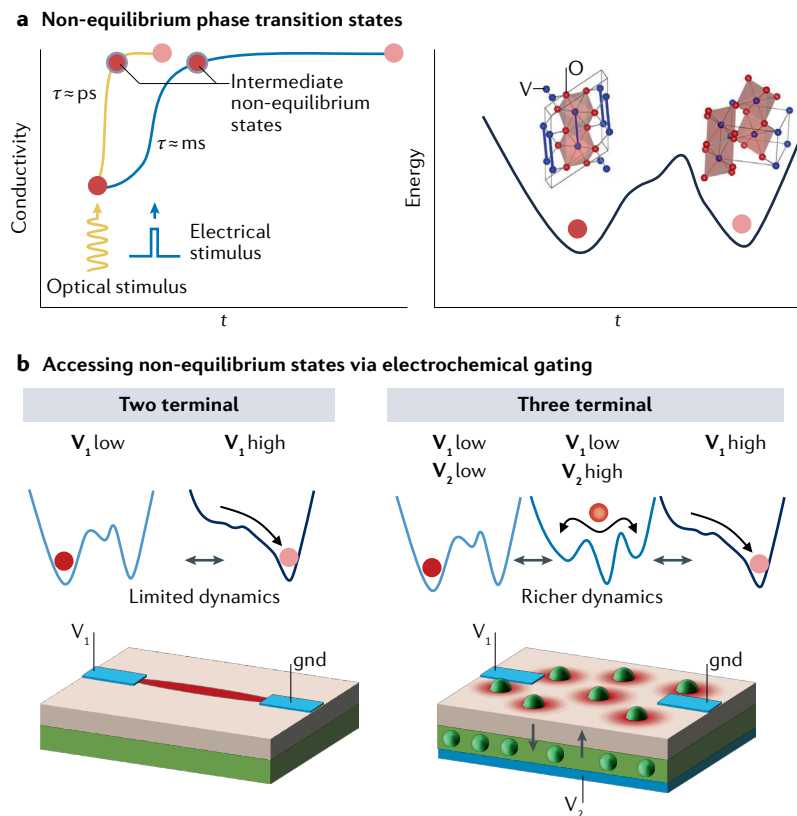


Fig. 7 | Accessing non-equilibrium phases. **a** | Non-equilibrium phase transition states in VO_2 , where the phase transition involves both an electronic and a crystal structure change. The kinetic pathway of the phase transition involves an intermediate state that is transformed in the electronic state but not in the crystal structure (labelled 'intermediate non-equilibrium states'). This kinetic pathway is identical upon both electrical and optical triggering, but the phase transition timescales resulting from the two triggering mechanisms differ by 12 orders of magnitude¹⁶⁰. **b** | Electrochemical means of accessing phase transitions and intermediate states. The illustration depicts a two-terminal device, similar to the case in panel **a**, where the intermediate state may be accessed only as a metastable state. However, using a third terminal and exploiting electrochemical tuning, it may be possible to access and stabilize intermediate phases, thereby leading to richer dynamics. *gnd*, electrical ground; *t*, temperature.

of such phase transitions were neglected as long as the transition was faster than the circuit timescales, although such dynamics have attracted scientific interest for decades. Given the increased interest in device dynamics and complexity, the technological relevance of phase transitions is now driving their study.

As an example, it was recently shown¹⁶⁰ that the Mott transition in VO_2 (which includes both an electronic and a structural change) takes an identical kinetic pathway upon both electrical and optical excitation. Both kinetic pathways contain the same starting and ending states (that differ in both electrical conductivity and crystal structure) and an intermediate state that is transformed in electrical conductivity, but not in crystal structure (FIG. 7a). However, the two pathways have timescales that differ by 12 orders of magnitude (picoseconds versus milliseconds). Such studies of intermediate non-equilibrium states and their properties (such as timescales, energy barriers and thermal properties)^{161,162} can be useful in guiding the design and manufacturing of future complex computing chips that employ phase

transitions. For example, such studies can inform the design process of device-level dynamics, the fundamental limits on the timescales, limits on the energy to traverse the known kinetics and aid in the choice of stimulating signals (electrical versus optical).

Electrochemical gating

Two-terminal memristors have an inherent fundamental limitation: the switching of states, volatile or non-volatile, is, by definition, a non-equilibrium runaway process. Some temporal control over the switching may lead to the stabilization and access of non-equilibrium and potentially interesting dynamical states.

Electrochemical gating via another terminal, which is the field-driven injection of dopants (defects or ions) near equilibrium, can modulate a material's resistance, crystal structure, stoichiometry and carrier concentration. The idea is not new, but it is now a potential means to access multiple dynamical processes, such as in phase transitions, which may otherwise be obscured in two-terminal devices within non-equilibrium intermediate states (FIG. 7b). In fact, it was shown¹⁶³ that electrochemical gating of TiO_2 using oxygen vacancies from yttria-stabilized zirconia enabled both phase coexistence (during the phase transition) and linearly programmable intermediate resistance states useful for bio-inspired computing^{164,165}.

Dynamics of filaments

The dynamics of a conduction channel or 'filament' (such as oxygen vacancy channels in non-volatile oxide memristors and metallic channels in volatile Mott memristors) have often been modelled as an order of complexity, mostly empirically. The origin of channel formation, its dynamics and the factors influencing them have not been understood to any appreciable extent. Recent postulates suggest that the separation of a hot channel region and the cold surrounding region in a memristor is thermodynamically favourable under certain conditions¹⁶⁶, which is why channels form, similar to how a mixture of oil and water separates via spinodal decomposition. This postulate implies an associated dynamics (and complexity) of such filament formation, but these dynamics are still unexplored.

There is also contention that runaway processes due to spatial temperature gradients lead to channels, a purely thermal process¹⁶⁷. Such models have reproduced experimental behaviours. Whether channel dynamics are driven by thermal, thermodynamic or any other process, they determine the nature of the differential equations describing such dynamics, which, in turn, inform device design. Thus, this topic is an important research avenue.

Local activity in ferromagnetic and ferroelectric materials

The concept of local activity (the ability of an otherwise passive system to amplify fluctuations to the input) has been successfully realized in volatile memristors via negative differential resistance. In fact, such an amplification is why volatile memristors can sustain oscillations in a relaxation circuit (as we discussed in the section on

second-order neuronal memristors). Over the past decade, there have been several reports of negative differential capacitance^{168,169}, especially in ferroelectric oxides of Pb–Zr–Ti. Further, negative differential inductance was reported in ferromagnetic materials¹⁷⁰. However, it is unclear whether such negative differential behaviours are associated with an order of complexity of their own. Creating self-sustained oscillations from such a behaviour will establish an order of complexity and enable the use of ferroelectric and ferromagnetic materials in complex systems.

Thermal dynamics

Temperature effects are universal in all of electronics. Thermal fluctuations can potentially add complexity by externally driving a system that is sensitive to thermal changes (especially nanoscale devices, owing to their small thermal mass); this was the case in nanoscale NbO₂ memristors driven into chaos by thermal fluctuations¹¹⁹. Further, the thermal conductances of Mott insulators such as VO₂ and NbO₂ change in anomalous ways, which are not fully understood, during their insulator–metal phase transitions¹⁷¹. It was argued that anomalous thermal changes in NbO₂ result in a new form of static current–voltage relationship¹⁷², and that such current–voltage behaviour may lead to a new order of complexity, resulting in neuron-like dynamics⁴⁷. Thermal dynamics, both internal and external to devices, are important to understand, not only to enable complexity in computing but to aid design of nearly all future electronic devices.

Modelling of complex electronic dynamics

Oscillations (some of the simplest complex dynamics) are ubiquitous in electronic circuits. Although there are necessary criteria (such as the Barkhausen and Nyquist stability criteria), there is no simple formulation of both necessary and sufficient criteria to predict oscillations¹⁷³. Likewise for higher-order dynamics, such as chaos. Bridging this gap requires elaborate numerical simulations and highlights the urgent need to develop robust predictive models for complex dynamics. Such predictive models will ease the design and integration of nanoscale and non-linear components (especially those that are prone to complex dynamics, such as memristors) onto sophisticated electronic chips. Leon Chua's theories of local activity, stability and chaos^{45,46,60} provide a solid, although purely mathematical, foundation, which electrical engineers can use to build physically realistic predictive models of complex dynamics with measurable parameters.

Future perspectives

We have reviewed a variety of complex dynamical properties, along with some of their potential computing applications. This Review has a materials and device focus, but any hardware implementation will require equal efforts at other levels of the computing stack, including architectures and system design, algorithms, compilers and other software tools. Although detailing the work in these areas is beyond the scope of this Review, we stress that a simultaneous co-design is critical

to fully leverage the dynamical and adapting capabilities of the core devices and materials. Further development is needed of the overlying computing models that leverage, and are compatible with, the dynamic evolution of the underlying computing and memory elements. In this regard, brain-inspired machine-learning models, cellular neural networks, evolutionary algorithms, Ising models and so on^{174–176} already provide a rich framework. In this section, we sidestep the fine details of the computing stack and forecast instead the most promising applications, particularly in comparison with other computing approaches.

A natural comparison is to existing mainstream digital von Neumann computing architectures, which include CPUs and GPUs. These technologies continue to progress, especially as new interconnects, 3D integration and novel packaging approaches help mitigate some of the challenges related to the von Neumann architecture. Another comparison is to the emerging area of quantum computing and quantum information processing²³. Other computing approaches are also emerging, such as optical or photonics-based, carbon-based and biomolecular computing^{24,25,29,177}. We discuss quantum computing in particular to offer an illustrative contrast in terms of power, form factor and target computing applications.

Modern computing hardware excels at highly sequential, high-precision and low-memory-bandwidth operations. Parallelism has been greatly expanded thanks to the development of GPUs, but is still challenged by high-memory-intensity workloads owing to limited bandwidth in available hardware platforms¹⁷⁸. Over the past 70 years, von Neumann-based hardware has been built on scales that go from low-power embedded systems up to exaflop supercomputers, with the power envelope spanning similar orders of magnitudes. Engineering across such scales is built upon rigid layers of abstraction between devices and circuits, up to software layers. Such a rigid hierarchy requires firm guarantees in precision, device yields, device characteristics, material defects and stable behaviour over the lifetime of the hardware. A consequence, as noted in the introduction, is that hardware primarily transforms inputs to new outputs, with learning and adaptation occurring primarily above the hardware layers, in the algorithms and software. The result is universal Turing completeness and the ability to tackle any workload, but in a way that is energy-inefficient and well suited only for sequential workloads that demand high precision (FIG. 8, yellow).

Quantum computing hopes to achieve exponential advantages over classical computing in some areas through the use of quantum bits that could explore an exponentially large Hilbert space through superposition and novel compute operations enabled by entanglement^{179,180}. Maintaining quantum coherence, required for such processes, requires the strictest constraints on the underlying quantum devices and cryogenic temperatures in many potential implementations, thereby resulting in high power and large form factors (FIG. 8, red). Similar to classical computing today, no higher-order dynamics or complex adaptation are

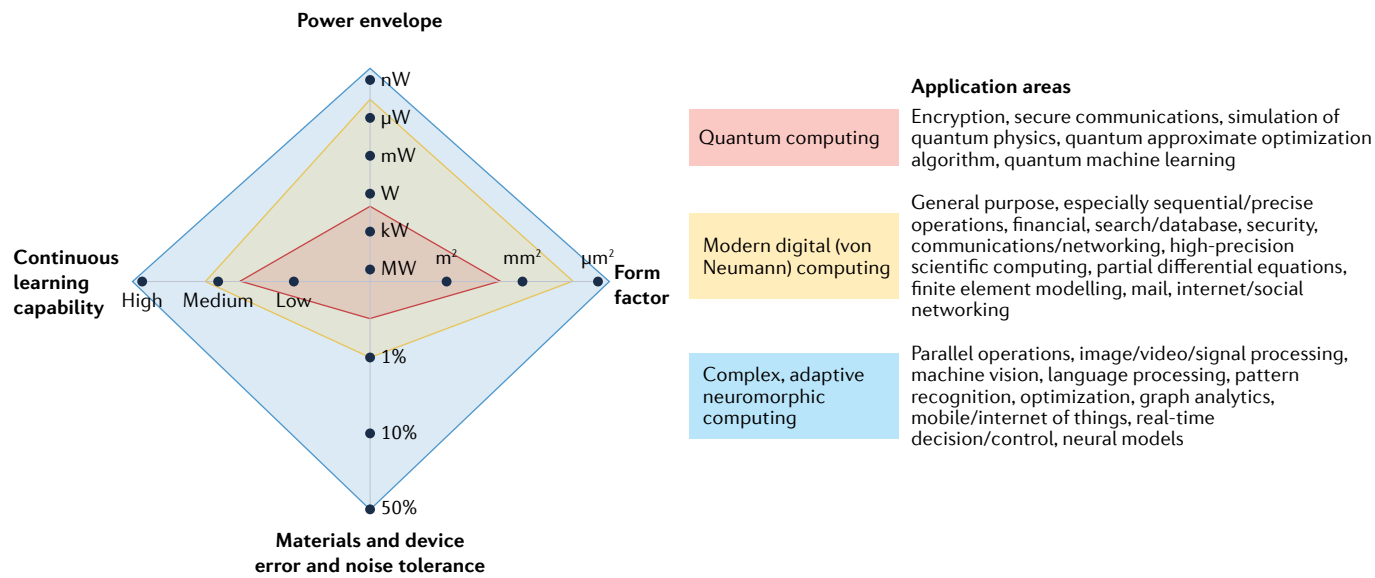


Fig. 8 | Comparison between the future requirements and potential of the main computing technologies. Projection of the measurable performance and attributes of three different computing technologies — modern digital computing, quantum computing and neuromorphic computing — for the next three decades and their potential applications.

targeted in the underlying hardware. The application areas driving the most interest are the unwinding of today's RSA (Rivest–Shamir–Adleman) encryption schemes and their replacement with truly secure quantum encryption¹⁸¹. The most promising applications are likely simulations of arbitrary quantum systems, such as in quantum chemistry and highly correlated electron systems^{182,183}. There is also ambitious research to develop quantum machine learning¹⁸⁴ and quantum optimization approaches¹⁸⁵, but quantifying clear advantages for a quantum computer is still work in progress. Additionally, the timeline for the engineering of a quantum computer with a sufficient number of logical qubits with low errors may be over a decade¹⁸⁶. An exponential advantage would be worth the wait; yet, we believe that the development of higher-complexity neuromorphic hardware can offer nearer-term advantages in complementary application areas.

The incorporation of highly complex dynamics and adaptation in bio-inspired computing is not expected to replace all forms of computing but, rather, to augment and complement them in a powerful way. In particular, many of the areas where traditional von Neumann systems excel, such as inherently serial workloads, will not be targeted. Instead, this novel form of computing will offer increased parallelism in areas such as pattern recognition and graph analytics. The coupling of computing and memory in non-von Neumann systems will allow ultra-low power and form factors (FIG. 8, blue), particularly well suited to the era of mobile and embedded systems. At the same time, this approach is fundamentally compatible with scale-up and scale-out and, thus, can tackle exascale-level computing workloads. Biological brains, similarly, can perform computations on scales that span many orders of magnitude³⁰. Key differentiators in bio-inspired computing will be the robustness to device and material defects, variability, stochasticity and low precision. The ability to adapt to

the local environment, including to defects and noise, is what enables flexibility, in addition to driving continuous learning and supporting computing applications requiring real-time control and decision-making (that is, adaptation). Naturally, bio-inspired computing hardware will be well matched to perform large-scale biological modelling needed in computational neuroscience and medicine. Developing and testing theories of neurophysiological models is of high interest; for example, understanding how neurons communicate with muscles¹⁸⁷ is an important problem to resolve in order to address neuromuscular diseases, such as amyotrophic lateral sclerosis. Such processes are challenging to simulate at large scales and with complex neuron models, thereby offering a unique niche for the initial deployment of bio-inspired hardware. Afterwards, the reduced precision, low latency and energy efficiency of bio-inspired hardware will make it well matched to accelerate many heuristics-based optimization algorithms, offering a path to tackling some of today's most computationally intractable problems¹⁷⁶.

Developing higher-complexity dynamical computing devices and materials brings together disparate areas of research into a single organized theme. This field is still young, especially at the architectural and algorithmic levels, but has remarkable potential. Over the next 10 years, we anticipate significant research into the development and applications of memristor dynamics of varying complexities, particularly motivated by biomimicry. We advocate for coordinated efforts among the many communities that have traditionally operated at distinct layers of the computing stack. Such synergy will be extremely beneficial to researchers in materials development, chip design, system integration, neuroscience, medicine and software.

Published online 8 April 2022

1. Moore, G. E. Cramming more components onto integrated circuits. *Electronics* **38**, 114–117 (1965).
2. Kendall, J. D. & Kumar, S. The building blocks of a brain-inspired computer. *Appl. Phys. Rev.* **7**, 011305 (2020).
3. Theis, T. N. & Wong, H.-S. P. The end of Moore's law: A new beginning for information technology. *Comput. Sci. Eng.* **19**, 41–50 (2017).
4. Alexander, F. et al. Exascale applications: skin in the game. *Philos. Trans. R. Soc. A* **378**, 20190056 (2020).
5. Messina, P. The exascale computing project. *Comput. Sci. Eng.* **19**, 63–67 (2017).
6. Leiserson, C. E. et al. There's plenty of room at the top: What will drive computer performance after Moore's law? *Science* **368**, eaam9744 (2020).
7. Lee, C. T. & Amaro, R. E. Exascale computing: A new dawn for computational biology. *Comput. Sci. Eng.* **20**, 18–25 (2018).
8. Schmidt, B. & Hildebrandt, A. Next-generation sequencing: big data meets high performance computing. *Drug Discov. Today* **22**, 712–717 (2017).
9. Wong, H.-S. P. et al. A density metric for semiconductor technology. *Proc. IEEE* **108**, 478–482 (2020).
10. Williams, R. S. What's next? The end of Moore's law. *Comput. Sci. Eng.* **19**, 7–13 (2017).
11. Chen, A. et al. A survey on architecture advances enabled by emerging beyond-CMOS technologies. *IEEE Des. Test* **36**, 46–68 (2019).
12. Dragoman, M. & Dragoman, D. *Atomic-Scale Electronics Beyond CMOS* (Springer, 2021).
13. Upadhyay, N. K. et al. Emerging memory devices for neuromorphic computing. *Adv. Mater. Technol.* **4**, 1800589 (2019).
14. Hebb, D. O. *The Organization of Behavior: A Neuropsychological Theory* (Wiley, 1949).
15. Rosenblatt, F. The perceptron: a probabilistic model for information storage and organization in the brain. *Psychol. Rev.* **65**, 386 (1958).
16. Ivakhnenko, A. G. & Lapa, V. G. *Cybernetics and Forecasting Techniques* Vol. 8 (American Elsevier, 1967).
17. Werbos, P. J. *Beyond Regression: New Tools for Prediction and Analysis in the Behavioral Sciences* (Harvard Univ., 1975).
18. Kelley, H. J. Gradient theory of optimal flight paths. *ARS J.* **30**, 947–954 (1960).
19. Rumelhart, D. E., Hinton, G. E. & Williams, R. J. Learning representations by back-propagating errors. *Nature* **323**, 533–536 (1986).
20. Hopfield, J. J. Neural networks and physical systems with emergent collective computational abilities. *Proc. Natl. Acad. Sci. USA* **79**, 2554–2558 (1982).
21. Kohonen, T. Self-organized formation of topologically correct feature maps. *Biol. Cybern.* **43**, 59–69 (1982).
22. Manipatruni, S., Nikonorov, D. E. & Young, I. A. Beyond CMOS computing with spin and polarization. *Nat. Phys.* **14**, 338–343 (2018).
23. Preskill, J. Quantum computing in the NISQ era and beyond. *Quantum* **2**, 79 (2018).
24. Solli, D. R. & Jalali, B. Analog optical computing. *Nat. Photonics* **9**, 704–706 (2015).
25. Paun, G., Rozenberg, G. & Salomaa, A. *DNA Computing: New Computing Paradigms* (Springer, 2005).
26. Mead, C. Neuromorphic electronic systems. *Proc. IEEE* **78**, 1629–1636 (1990).
27. Kephart, J. O. & Chess, D. M. The vision of autonomic computing. *Computer* **36**, 41–50 (2003).
28. Kish, L. B. Thermal noise driven computing. *Appl. Phys. Lett.* **89**, 144104 (2006).
29. Unger, R. & Moult, J. Towards computing with proteins. *Proteins* **63**, 53–64 (2006).
30. Herculano-Houzel, S. *The Human Advantage: A New Understanding of How Our Brain Became Remarkable* (MIT Press, 2016).
31. Mead, C. How we created neuromorphic engineering. *Nat. Electron.* **3**, 434–435 (2020).
32. James, C. D. et al. A historical survey of algorithms and hardware architectures for neural-inspired and neuromorphic computing applications. *Biol. Inspired Cogn. Archit.* **19**, 49–64 (2017).
33. McCulloch, W. S. & Pitts, W. A logical calculus of the ideas immanent in nervous activity. *Bull. Math. Biophys.* **5**, 115–133 (1943).
34. Pitts, W. Some observations on the simple neuron circuit. *Bull. Math. Biophys.* **4**, 121–129 (1942).
35. Hodgkin, A. L. & Huxley, A. F. A quantitative description of membrane current and its application to conduction and excitation in nerve. *J. Physiol.* **117**, 500–544 (1952).
36. FitzHugh, R. Impulses and physiological states in theoretical models of nerve membrane. *Biophys. J.* **1**, 445–466 (1961).
37. Nagumo, J., Arimoto, S. & Yoshizawa, S. An active pulse transmission line simulating nerve axon. *Proc. IRE* **50**, 2061–2070 (1962).
38. Dayhoff, J. E. *Neural Network Architectures: An Introduction* (Van Nostrand Reinhold, 1990).
39. Bengio, Y. in *Proceedings of ICML Workshop on Unsupervised and Transfer Learning* (eds Guyon, I., Dror, G., Lemire, V., Taylor, G. & Silver, D.) 17–36 (PMLR, 2012).
40. Schmidhuber, J. Deep learning in neural networks: An overview. *Neural Netw.* **61**, 85–117 (2015).
41. Izhikevich, E. M. Which model to use for cortical spiking neurons? *IEEE Trans. Neural Netw.* **15**, 1063–1070 (2004).
42. Turing, A. M. in *The Turing Test: Verbal Behavior as the Hallmark of Intelligence* (ed. Shieber, S. M.) 110–127 (MIT Press, 1964).
43. Gell-Mann, M. in *Complexity and Industrial Clusters* (eds Curzio, Q. & Fortis, M.) 13–24 (Springer, 2002).
44. Adami, C. What is complexity? *BioEssays* **24**, 1085–1094 (2002).
45. Chua, L. O. CNN: A vision of complexity. *Int. J. Bifurc. Chaos* **7**, 2219–2425 (1997).
46. Chua, L. O. Local activity is the origin of complexity. *Int. J. Bifurc. Chaos* **15**, 3435–3456 (2005).
47. Kumar, S., Williams, R. S. & Wang, Z. Third-order nanocircuit elements for neuromorphic engineering. *Nature* **585**, 518–523 (2020).
48. Csete, M. E. & Doyle, J. C. Reverse engineering of biological complexity. *Science* **295**, 1664–1669 (2002).
49. Solé, R. & Goodwin, B. *Signs of Life: How Complexity Pervades Biology* (Basic Books, 2000).
50. Bonchev, D. D. & Rouvray, D. *Complexity in Chemistry, Biology, and Ecology* (Springer, 2007).
51. Whitesides, G. M. & Ismagilov, R. F. Complexity in chemistry. *Science* **284**, 89–92 (1999).
52. Stanley, H. et al. Self-organized complexity in economics and finance. *Proc. Natl. Acad. Sci. USA* **99**, 2561–2565 (2002).
53. Arthur, W. B. Foundations of complexity economics. *Nat. Rev. Phys.* **3**, 136–145 (2021).
54. Hannerz, U. *Cultural Complexity: Studies in the Social Organization of Meaning* (Columbia Univ. Press, 1992).
55. Freeberg, T. M., Dunbar, R. I. & Ord, T. J. Social complexity as a proximate and ultimate factor in communicative complexity. *Philos. Trans. R. Soc. B Biol. Sci.* **367**, 1785–1801 (2012).
56. Magee, J. C. & Grienberger, C. Synaptic plasticity forms and functions. *Annu. Rev. Neurosci.* **43**, 95–117 (2020).
57. Eccles, J. C. *The Physiology of Synapses* (Academic Press, 2013).
58. Fain, G. L. *Molecular and Cellular Physiology of Neurons* (Harvard Univ. Press, 1999).
59. Hopfield, J. J. Neurons, dynamics and computation. *Phys. Today* **47**, 40–47 (1994).
60. Mainzer, K. & Chua, L. *Local Activity Principle: The Cause of Complexity and Symmetry Breaking* (World Scientific, 2013).
61. Chua, L. O. & Lin, T. Chaos and fractals from third-order digital filters. *Int. J. Circuit Theory Appl.* **18**, 241–255 (1990).
62. Barrio, R., Martínez, M. A., Serrano, S. & Wilczak, D. When chaos meets hyperchaos: 4D Rössler model. *Phys. Lett. A* **379**, 2300–2305 (2015).
63. Koch, C. & Poggio, T. in *Single Neuron Computation* (eds McKenna, T., Davis, J. & Zornetzer, S. F.) 315–345 (Elsevier, 1992).
64. Izhikevich, E. M. Simple model of spiking neurons. *IEEE Trans. Neural Netw.* **14**, 1569–1572 (2003).
65. Wilson, H. R. Voluntary generation of hyperchaotic visuo-motor patterns. *Sci. Rep.* **9**, 13819 (2019).
66. Nawrocki, R. A., Voyles, R. M. & Shaheen, S. E. A mini review of neuromorphic architectures and implementations. *IEEE Trans. Electron Devices* **63**, 3819–3829 (2016).
67. He, Y. et al. Recent progress on emerging transistor-based neuromorphic devices. *Adv. Intell. Syst.* **3**, 2000210 (2021).
68. Chua, L. Memristor—the missing circuit element. *IEEE Trans. Circuit Theory* **18**, 507–519 (1971).
69. Strukov, D. B., Snider, G. S., Stewart, D. R. & Williams, R. S. The missing memristor found. *Nature* **453**, 80–83 (2008).
70. Pickett, M. D., Medeiros-Ribeiro, G. & Williams, R. S. A scalable neuristor built with Mott memristors. *Nat. Mater.* **12**, 114–117 (2013).
71. Zhu, M., Ren, K. & Song, Z. Onvonic threshold switching selectors for three-dimensional stackable phase-change memory. *MRS Bull.* **44**, 715–720 (2019).
72. Wang, Z. et al. Memristors with diffusive dynamics as synaptic emulators for neuromorphic computing. *Nat. Mater.* **16**, 101–108 (2017).
73. Kumar, S. et al. Direct observation of localized radial oxygen migration in functioning tantalum oxide memristors. *Adv. Mater.* **28**, 2772–2776 (2016).
74. Pershin, Y. V. & Di Ventra, M. Spin memristive systems: Spin memory effects in semiconductor spintronics. *Phys. Rev. B* **78**, 113309 (2008).
75. Endoh, T., Koike, H., Ikeda, S., Hanyu, T. & Ohno, H. An overview of nonvolatile emerging memories—spintronics for working memories. *IEEE J. Emerg. Sel. Topics Circuits Syst.* **6**, 109–119 (2016).
76. Meena, J. S., Sze, S. M., Chand, U. & Tseng, T.-Y. Overview of emerging nonvolatile memory technologies. *Nanoscale Res. Lett.* **9**, 526 (2014).
77. Raoux, S., Xiong, F., Wuttig, M. & Pop, E. Phase change materials and phase change memory. *MRS Bull.* **39**, 703–710 (2014).
78. Choi, S., Yang, J. & Wang, G. Emerging memristive artificial synapses and neurons for energy-efficient neuromorphic computing. *Adv. Mater.* **32**, 2004659 (2020).
79. Guo, R., Lin, W., Yan, X., Venkatesan, T. & Chen, J. Ferroic tunnel junctions and their application in neuromorphic networks. *Appl. Phys. Rev.* **7**, 011304 (2020).
80. Li, Y., Wang, Z., Midya, R., Xia, Q. & Yang, J. J. Review of memristor devices in neuromorphic computing: materials sciences and device challenges. *J. Phys. D Appl. Phys.* **51**, 503002 (2018).
81. Zidan, M. A., Strachan, J. P. & Lu, W. D. The future of electronics based on memristive systems. *Nat. Electron.* **1**, 22–29 (2018).
82. Sun, K., Chen, J. & Yan, X. The future of memristors: materials engineering and neural networks. *Adv. Funct. Mater.* **31**, 2006773 (2021).
83. Xu, W., Wang, J. & Yan, X. Advances in memristor-based neural networks. *Front. Nanotechnol.* **3**, 645995 (2021).
84. Kim, M.-K., Park, Y., Kim, I.-J. & Lee, J.-S. Emerging materials for neuromorphic devices and systems. *Iscience* **23**, 101846 (2020).
85. Wang, C.-Y. et al. 2D layered materials for memristive and neuromorphic applications. *Adv. Electron. Mater.* **6**, 1901107 (2020).
86. Krestinskaya, O., James, A. P. & Chua, L. O. Neuromemristive circuits for edge computing: A review. *IEEE Trans. Neural Netw. Learn. Syst.* **31**, 4–23 (2019).
87. Goi, E., Zhang, O., Chen, X., Luan, H. & Gu, M. Perspective on photonic memristive neuromorphic computing. *Photonix* **1**, 3 (2020).
88. Mao, J.-Y., Zhou, L., Zhu, X., Zhou, Y. & Han, S.-T. Photonic memristor for future computing: a perspective. *Adv. Opt. Mater.* **7**, 1900766 (2019).
89. Sangwan, V. K. & Hersam, M. C. Neuromorphic nanoelectronic materials. *Nat. Nanotechnol.* **15**, 517–528 (2020).
90. Sokolov, A. S., Abbas, H., Abbas, Y. & Choi, C. Towards engineering in memristors for emerging memory and neuromorphic computing: a review. *J. Semicond.* **42**, 013101 (2021).
91. Islam, R. et al. Device and materials requirements for neuromorphic computing. *J. Phys. D Appl. Phys.* **52**, 113001 (2019).
92. Jeong, D. S. & Hwang, C. S. Nonvolatile memory materials for neuromorphic intelligent machines. *Adv. Mater.* **30**, 1704729 (2018).
93. del Valle, J., Ramírez, J. G., Rozenberg, M. J. & Schuller, I. K. Challenges in materials and devices for resistive-switching-based neuromorphic computing. *J. Appl. Phys.* **124**, 211101 (2018).
94. Burr, G. W., Sebastian, A., Vianello, E., Waser, R. & Parkin, S. Emerging materials in neuromorphic computing: Guest editorial. *APL Mater.* **8**, 010401 (2020).
95. Wang, Z. et al. Resistive switching materials for information processing. *Nat. Rev. Mater.* **5**, 173–195 (2020).
96. Zhang, W. et al. Neuro-inspired computing chips. *Nat. Electron.* **3**, 371–382 (2020).
97. Mehonic, A. et al. Memristors — from in-memory computing, deep learning acceleration, and spiking neural networks to the future of neuromorphic and bio-inspired computing. *Adv. Intell. Syst.* **2**, 2000085 (2020).
98. Sung, C., Hwang, H. & Yoo, I. K. Perspective: A review on memristive hardware for neuromorphic computation. *J. Appl. Phys.* **124**, 151903 (2018).
99. Wang, H. & Yan, X. Overview of resistive random access memory (RRAM): materials, filament mechanisms,

performance optimization, and prospects. *Phys. Status Solidi Rapid Res. Lett.* **13**, 1900073 (2019).

100. Hong, X. et al. Oxide-based RRAM materials for neuromorphic computing. *J. Mater. Sci.* **53**, 8720–8746 (2018).
101. Moon, K. et al. RRAM-based synapse devices for neuromorphic systems. *Faraday Discuss.* **213**, 421–451 (2019).
102. Chen, Y. ReRAM: History, status, and future. *IEEE Trans. Electron Devices* **67**, 1420–1433 (2020).
103. Shen, Z. et al. Advances of RRAM devices: Resistive switching mechanisms, materials and bionic synaptic application. *Nanomaterials* **10**, 1437 (2020).
104. Banerjee, W. Challenges and applications of emerging nonvolatile memory devices. *Electronics* **9**, 1029 (2020).
105. Rehman, M. M. et al. Decade of 2D-materials-based RRAM devices: a review. *Sci. Technol. Adv. Mater.* **21**, 147–186 (2020).
106. Feng, X., Liu, X. & Ang, K.-W. 2D photonic memristor beyond graphene: progress and prospects. *Nanophotonics* **9**, 1579–1599 (2020).
107. Wang, Y. et al. Mott-transition-based RRAM. *Mater. Today* **28**, 63–80 (2019).
108. Goswami, S., Goswami, S. & Venkatesan, T. An organic approach to low energy memory and brain inspired electronics. *Appl. Phys. Rev.* **7**, 021303 (2020).
109. van De Burgt, Y., Melianas, A., Keene, S. T., Malliaras, G. & Salleo, A. Organic electronics for neuromorphic computing. *Nat. Electron.* **1**, 386–397 (2018).
110. Ahn, E. C., Wong, H.-S. P. & Pop, E. Carbon nanomaterials for non-volatile memories. *Nat. Rev. Mater.* **3**, 18009 (2018).
111. Kim, S. et al. Experimental demonstration of a second-order memristor and its ability to biorealistically implement synaptic plasticity. *Nano Lett.* **15**, 2203–2211 (2015).
112. Rodríguez-Fernández, A., Cagli, C., Perniola, L., Miranda, E. & Sufián, J. Characterization of HfO_2 -based devices with indication of second order memristor effects. *Microelectron. Eng.* **195**, 101–106 (2018).
113. Mikheev, V. et al. Ferroelectric second-order memristor. *ACS Appl. Mater. Interfaces* **11**, 32108–32114 (2019).
114. Slesazeck, S. & Mikolajick, T. Nanoscale resistive switching memory devices: a review. *Nanotechnology* **30**, 352003 (2019).
115. Chen, A. A review of emerging non-volatile memory (NVM) technologies and applications. *Solid State Electron.* **125**, 25–38 (2016).
116. Alexandrov, A. et al. Current-controlled negative differential resistance due to Joule heating in TiO_2 . *Appl. Phys. Lett.* **99**, 202104 (2011).
117. Pickett, M. D., Borghetti, J., Yang, J. J., Medeiros-Ribeiro, G. & Williams, R. S. Coexistence of memristance and negative differential resistance in a nanoscale metal-oxide-metal system. *Adv. Mater.* **23**, 1730–1733 (2011).
118. Narayanan, V., Li, J.-S. & Ching, S. Biophysically interpretable inference of single neuron dynamics. *J. Comput. Neurosci.* **47**, 61–76 (2019).
119. Kumar, S., Strachan, J. P. & Williams, R. S. Chaotic dynamics in nanoscale NbO_2 Mott memristors for analogue computing. *Nature* **548**, 318–321 (2017).
120. Yi, W. et al. Biological plausibility and stochasticity in scalable VO_2 active memristor neurons. *Nat. Commun.* **9**, 4661 (2018).
121. Fitch, A. L., Yu, D., Iu, H. H. & Sreeram, V. Hyperchaos in a memristor-based modified canonical Chua's circuit. *Int. J. Bifurc. Chaos* **22**, 1250133 (2012).
122. Ercsey-Ravasz, M. & Toroczkai, Z. Optimization hardness as transient chaos in an analog approach to constraint satisfaction. *Nat. Phys.* **7**, 966–970 (2011).
123. Yu, W. et al. Design of a new seven-dimensional hyperchaotic circuit and its application in secure communication. *IEEE Access* **7**, 125586–125608 (2019).
124. An, X., Jiang, M., Deng, W. & Fang, J. A novel dual memristor hyperchaotic system and its application for secure communication based on three-fold function projection synchronization. *Int. J. Numer. Model. Electron. Netw. Devices Fields* **34**, e2825 (2021).
125. Wang, Z., Min, F. & Wang, E. A new hyperchaotic circuit with two memristors and its application in image encryption. *AIP Adv.* **6**, 095316 (2016).
126. Wang, L., Dong, T. & Ge, M.-F. Finite-time synchronization of memristor chaotic systems and its application in image encryption. *Appl. Math. Comput.* **347**, 293–305 (2019).
127. Ruan, J., Sun, K., Mou, J., He, S. & Zhang, L. Fractional-order simplest memristor-based chaotic circuit with new derivative. *Eur. Phys. J.* **133**, 3 (2018).
128. Zhu, J. L., Dong, J. & Gao, H. Q. Nine-dimensional eight-order chaotic system and its circuit implementation. *Appl. Mech. Mater.* **716**, 1346–1351 (2015).
129. Zhang, Y. et al. Brain-inspired computing with memristors: Challenges in devices, circuits, and systems. *Appl. Phys. Rev.* **7**, 011308 (2020).
130. Caravelli, F. & Carbajal, J. P. Memristors for the curious outsiders. *Technologies* **6**, 118 (2018).
131. Chu, M. et al. Neuromorphic hardware system for visual pattern recognition with memristor array and CMOS neuron. *IEEE Trans. Ind. Electron.* **62**, 2410–2419 (2014).
132. Zidan, M. A. et al. A general memristor-based partial differential equation solver. *Nat. Electron.* **1**, 411–420 (2018).
133. Wang, Z. et al. In situ training of feed-forward and recurrent convolutional memristor networks. *Nat. Mach. Intell.* **1**, 434–442 (2019).
134. Wang, Z. et al. Fully memristive neural networks for pattern classification with unsupervised learning. *Nat. Electron.* **1**, 137–145 (2018).
135. Sebastian, A. et al. Temporal correlation detection using computational phase-change memory. *Nat. Commun.* **8**, 1115 (2017).
136. Yu, Y. et al. In-memory realization of eligibility traces based on conductance drift of phase change memory for energy-efficient reinforcement learning. *Adv. Mater.* **34**, 2107811 (2021).
137. Zidan, M. A., Jeong, Y. & Lu, W. D. Temporal learning using second-order memristors. *IEEE Trans. Nanotechnol.* **16**, 721–723 (2017).
138. Cai, F. et al. Power-efficient combinatorial optimization using intrinsic noise in memristor Hopfield neural networks. *Nat. Electron.* **3**, 409–418 (2020).
139. Diaz-Alvarez, A., Higuchi, R., Li, Q., Shingaya, Y. & Nakayama, T. Associative routing through neuromorphic nanowire networks. *AIP Adv.* **10**, 025134 (2020).
140. Sillin, H. O. et al. A theoretical and experimental study of neuromorphic atomic switch networks for reservoir computing. *Nanotechnology* **24**, 384004 (2013).
141. Diaz-Alvarez, A. et al. Emergent dynamics of neuromorphic nanowire networks. *Sci. Rep.* **9**, 14920 (2019).
142. Fu, K. et al. in *2020 International Joint Conference on Neural Networks (IJCNN)* 1–8 (IEEE, 2020).
143. Kuncic, Z. et al. in *2020 IEEE International Symposium on Circuits and Systems (ISCAS)* 1–5 (IEEE, 2020).
144. Zhu, R. et al. in *2020 International Conference on Rebooting Computing (ICRC)* 102–106 (IEEE, 2020).
145. Demis, E. C. et al. Atomic switch networks — nanoarchitectonic design of a complex system for natural computing. *Nanotechnology* **26**, 204003 (2015).
146. Lilak, S. et al. Spoken digit classification by in-materio reservoir computing with neuromorphic atomic switch networks. *Front. Nanotechnol.* **3**, 38 (2021).
147. Avizienis, A. V. et al. Neuromorphic atomic switch networks. *PLoS ONE* **7**, e42772 (2012).
148. Tanaka, G. et al. Recent advances in physical reservoir computing: A review. *Neural Netw.* **115**, 100–123 (2019).
149. Kuncic, Z. & Nakayama, T. Neuromorphic nanowire networks: principles, progress and future prospects for neuro-inspired information processing. *Adv. Phys. X* **6**, 1894234 (2021).
150. Pantone, R. D., Kendall, J. D. & Nino, J. C. Memristive nanowires exhibit small-world connectivity. *Neural Netw.* **106**, 144–151 (2018).
151. Du, C. et al. Reservoir computing using dynamic memristors for temporal information processing. *Nat. Commun.* **8**, 2204 (2017).
152. Moon, J. et al. Temporal data classification and forecasting using a memristor-based reservoir computing system. *Nat. Electron.* **2**, 480–487 (2019).
153. Torrejon, J. et al. Neuromorphic computing with nanoscale spintronic oscillators. *Nature* **547**, 428–431 (2017).
154. Zhu, X., Li, D., Liang, X. & Lu, W. D. Ionic modulation and ionic coupling effects in MoS_2 devices for neuromorphic computing. *Nat. Mater.* **18**, 141–148 (2019).
155. Yang, Y., Chen, B. & Lu, W. D. Memristive physically evolving networks enabling the emulation of heterosynaptic plasticity. *Adv. Mater.* **27**, 7720–7727 (2015).
156. Csaba, G. & Porod, W. Coupled oscillators for computing: A review and perspective. *Appl. Phys. Rev.* **7**, 011302 (2020).
157. Velichko, A., Belyaev, M., Putrolaynen, V., Perminov, V. & Pergament, A. Thermal coupling and effect of subharmonic synchronization in a system of two VO_2 based oscillators. *Solid State Electron.* **141**, 40–49 (2018).
158. Brown, K. R. et al. Coupled quantized mechanical oscillators. *Nature* **471**, 196–199 (2011).
159. Koppenhöfer, M., Bruder, C. & Roulet, A. Quantum synchronization on the IBM Q system. *Phys. Rev. Res.* **2**, 023026 (2020).
160. Sood, A. et al. Universal phase dynamics in VO_2 switches revealed by ultrafast operando diffraction. *Science* **373**, 352–355 (2021).
161. Laverock, J. et al. Direct observation of decoupled structural and electronic transitions and an ambient pressure monocliniclike metallic phase of VO_2 . *Phys. Rev. Lett.* **113**, 216402 (2014).
162. Kumar, S. et al. Sequential electronic and structural transitions in VO_2 observed using X-ray absorption spectromicroscopy. *Adv. Mater.* **26**, 7505–7509 (2014).
163. Li, Y. et al. Filament-free bulk resistive memory enables deterministic analogue switching. *Adv. Mater.* **32**, 2003984 (2020).
164. Fuller, E. J. et al. Parallel programming of an ionic floating-gate memory array for scalable neuromorphic computing. *Science* **364**, 570–574 (2019).
165. Zhu, J. et al. Ion gated synaptic transistors based on 2D van der Waals crystals with tunable diffusive dynamics. *Adv. Mater.* **30**, 1800195 (2018).
166. Kumar, S. & Williams, R. S. Separation of current density and electric field domains caused by nonlinear electronic instabilities. *Nat. Commun.* **9**, 2030 (2018).
167. Goodwill, J. M. et al. Spontaneous current constriction in threshold switching devices. *Nat. Commun.* **10**, 1628 (2019).
168. Íñiguez, J., Zubko, P., Luk'yanchuk, I. & Cano, A. Ferroelectric negative capacitance. *Nat. Rev. Mater.* **4**, 243–256 (2019).
169. Islam Khan, A. et al. Experimental evidence of ferroelectric negative capacitance in nanoscale heterostructures. *Appl. Phys. Lett.* **99**, 113501 (2011).
170. Kumar, S. & Williams, R. S. Tutorial: experimental nonlinear dynamical circuit analysis of a ferromagnetic inductor. *IEEE Circuits Syst. Mag.* **18**, 28–34 (2018).
171. Chen, L. et al. Enhancement of thermal conductivity across the metal-insulator transition in vanadium dioxide. *Appl. Phys. Lett.* **113**, 061902 (2018).
172. Kumar, S. et al. Physical origins of current and temperature controlled negative differential resistances in NbO_2 . *Nat. Commun.* **8**, 658 (2017).
173. von Wangenheim, L. On the Barkhausen and Nyquist stability criteria. *Analog Integr. Circuits Signal. Process.* **66**, 139–141 (2011).
174. Chua, L. O. & Yang, L. Cellular neural networks: Theory. *IEEE Trans. Circuits Syst.* **35**, 1257–1272 (1988).
175. Vikhar, P. A. in *2016 International Conference on Global Trends in Signal Processing, Information Computing and Communication (ICGTPICC)* 261–265 (IEEE, 2016).
176. Strachan, J. P. Fast Ising solvers based on oscillator networks. *Nat. Electron.* **4**, 458–459 (2021).
177. Shulaker, M. M. et al. Carbon nanotube computer. *Nature* **501**, 526–530 (2013).
178. Kogge, P. et al. *ExaScale Computing Study: Technology Challenges in Achieving Exascale Systems* (DARPA IPTO, 2008).
179. Freedman, M. H. P/NP, and the quantum field computer. *Proc. Natl. Acad. Sci. USA* **95**, 98–101 (1998).
180. Bennett, C. H., Bernstein, E., Brassard, G. & Vazirani, U. Strengths and weaknesses of quantum computing. *SIAM J. Comput.* **26**, 1510–1523 (1997).
181. Shor, P. W. Polynomial-time algorithms for prime factorization and discrete logarithms on a quantum computer. *SIAM Rev.* **41**, 303–332 (1999).
182. Feynman, R. P. in *Feynman and Computation* 133–153 (CRC Press, 2018).
183. Childs, A. M., Maslov, D., Nam, Y., Ross, N. J. & Su, Y. Toward the first quantum simulation with quantum speedup. *Proc. Natl. Acad. Sci. USA* **115**, 9456–9461 (2018).

184. Harrow, A. W., Hassidim, A. & Lloyd, S. Quantum algorithm for linear systems of equations. *Phys. Rev. Lett.* **103**, 150502 (2009).

185. Farhi, E., Goldstone, J. & Gutmann, S. A quantum approximate optimization algorithm. Preprint at <https://arxiv.org/abs/1411.4028> (2014).

186. Green, D., Soller, H., Oreg, Y. & Galitski, V. How to profit from quantum technology without building quantum computers. *Nat. Rev. Phys.* **3**, 150–152 (2021).

187. Bertuzzi, M., Chang, W. & Ampatzis, K. Adult spinal motoneurons change their neurotransmitter phenotype to control locomotion. *Proc. Natl. Acad. Sci. USA* **115**, 9926–9933 (2018).

Acknowledgements

The authors gratefully acknowledge S. M. Bohaichuk and R. S. Williams for feedback on the manuscript. S.K. was supported by the Laboratory Directed Research and Development programme at Sandia National Laboratories,

a multi-mission laboratory managed and operated by National Technology and Engineering Solutions of Sandia, LLC, a wholly owned subsidiary of Honeywell International Inc., for the U.S. Department of Energy's National Nuclear Security Administration under contract DE-NA0003525. This paper describes objective technical results and analysis. Any subjective views or opinions that might be expressed in the paper do not necessarily represent the views of the U.S. Department of Energy or the United States Government. Y.Y. acknowledges support from the National Key Research and Development Program of China (2017YFA0207600), National Natural Science Foundation of China (61925401, 92064004), projects 2019BD002 and 2020BD010 supported by PKU-Baidu Fund, the Fok Ying-Tong Education Foundation, Beijing Academy of Artificial Intelligence (BAAI) and the Tencent Foundation through the XPLORER PRIZE. X.W. and W.D.L. acknowledge financial support from the National Science Foundation through awards CCF-1900675 and DMR-1810119.

Author contributions

All the authors contributed to the conception of the ideas, literature review, writing of the manuscript, preparation of the figures and editing.

Competing interests

The authors declare no competing interests.

Peer review information

Nature Reviews Materials thanks Leon O. Chua, Mario Lanza and J. Joshua Yang for their contribution to the peer review of this work.

Publisher's note

Springer Nature remains neutral with regard to jurisdictional claims in published maps and institutional affiliations.

© Springer Nature Limited 2022